Spring 2017

Analysis and implementation of accident tolerant nuclear fuels

Benjamin Joseph Prewitt

Department:

Recommended Citation

Prewitt, Benjamin Joseph, "Analysis and implementation of accident tolerant nuclear fuels" (2017). *Masters Theses*. 7657.
http://scholarsmine.mst.edu/masters_theses/7657

ANALYSIS AND IMPLEMENTATION
OF ACCIDENT TOLERANT NUCLEAR FUELS

by

BENJAMIN JOSEPH PREWITT

A THESIS

Presented to the faculty of the Graduate School of the

MISSOURI UNIVERSITY OF SCIENCE AND TECHNOLOGY

In Partial Fulfillment of the Requirements for the Degree

MASTER OF SCIENCE IN NUCLEAR ENGINEERING

2017

Approved by

Ayodeji Alajo, Advisor

Carlos Castaño

Joshua Schlegel

ABSTRACT

To improve the reliability and robustness of LWR, accident tolerant nuclear fuels and cladding materials are being developed to possibly replace the current UO_2/zirconium system. This research highlights UN and U_3Si_2, two of the most favorable accident tolerant fuels being developed. To evaluate the commercial feasiblilty of these fuels, two areas of research were conducted. Chemical fabrication routes for both fuels were investigated in detail, considering UO_2 and UF_6 as potential starting materials. Potential pathways for industrial scale fabrication using these methods were discussed.

Neutronic performance of 70%UN-30%U_3Si_2 composite was evaluated in MNCP using PWR assembly and core models. The results showed comparable performance to an identical UO_2 fueled simulation with the same configuration. The parameters simulated for composite and oxide fuel include the following: fuel to moderator ratio curves; energy dependent flux spectra; temperature coefficients for fuel and moderator; delayed neutron fractions; power peaking factors; axial and radial flux profiles in 2D and 3D; burnup; critical boron concentration; and shutdown margin. Overall, the neutronic parameters suggest that the transition from UO_2 to composite in existing nuclear systems will not require significant changes in operating procedures or modifications to standards and regulations.

ACKNOWLEDGEMENTS

I would like express my profound thanks to Dr. Ayodeji Alajo for his guidance, suggestions, and support throughout the development of this work. I would also like to thank Dr. Carlos Castaño and Dr. Joshua Schlegel for taking the time to review my work as members of my graduate committee.

TABLE OF CONTENTS

Page

SECTION

APPENDICES

LIST OF FIGURES

Page

LIST OF TABLES

Page

NOMENCLATURE

ADU	Ammonium Diuranate
AFC	Advanced Fuels Campaign
AIC	Silver-Indium-Cadmium (Ag-In-Cd)
ATF	Accident Tolerant Fuel
CANDU	Canada Deuterium Uranium
DOE	Department of Energy
FPUL	Flux per Unit Lethargy
GRCA	Gray Rod Cluster Assembly
HLW	High Level Waste
LWR	Light Water Reactor
MTR	Materials Testing Reactor
PWR	Pressurized Water Reactor
RCCA	Reactivity Control Cluster Assembly
SNAP	Space Nuclear Auxiliary Power
SPFT	Special Purpose Fission Technology
TRISO	Tristructural Isotropic Particle Fuel

1. INTRODUCTION

The Department of Energy recently began a research initiative, known as the Advanced Fuels Campaign (AFC), to develop innovative fuel and cladding technology for current and next generation nuclear reactors. Corporate groups partnered with the DOE to design and fabricate the prototypes to be evaluated by Idaho National Laboratory in the laboratory's facilities. Primary objectives of the program consisted of demonstrating the performance of advanced fuel and cladding materials, and evaluating the methods for engineering scale production of these materials. The initiative sought to investigate alternative fuel cycles that achieve the following: improvements in efficiency, resource utilization, and burnup while minimizing proliferation risk, fabrication losses, and generation of HLW and UNF. [Maloy et al, 2014]

Following the 2011 events at the Fukushima Daiichi reactor facility, the focus of this program shifted to prioritize fuel reliability, safety, and performance in accident scenarios. Specifically, The Department of Energy was directed to "*give priority to developing enhanced fuels and cladding for light water reactors to improve safety in the event of accidents in the reactor spent fuel pools*" and to "*give special technical emphasis and funding priority to develop meltdown resistant, accident tolerant nuclear fuels that would enhance the safety of present and future generations of light water reactors*." [Braase, 2014]

The main category of accidents in a LWR involves or results in a loss of cooling. Inadequate heat removal can lead to fuel failure or melting, cladding damage or failure, and fission product release. Another consequence of a loss of cooling in a LWR is the oxidation of the cladding. When exposed to steam, zirconium cladding will oxidize at a rate that increases with temperature. This reaction produces hydrogen gas, and at the high temperatures of a loss of cooling accident, the hydrogen production contributes significantly to the increasing system pressure. This gas is also flammable and may ignite. These events have the potential to increase the pressure of a containment structure; which can potentially rupture the containment building, releasing radioactive material into the atmosphere.

To reduce or eliminate the potential for this kind of accident, several types of Accident Tolerant Fuel (ATF) are being developed. An accident tolerant fuel features improvements over conventional designs in the following areas of performance: better response to anticipated operational occurrences, design basis events, and beyond design basis events; and maintaining or improving current levels of performance, operations, and economics. [Maloy et al] Such a design will be an improved replacement of conventional uranium dioxide/zirconium fuel systems. The specific metrics for ATF candidate materials have been reported in detail by the INL researchers complete with a thorough evaluation and selection process. [Bragg-Sitton et al, 2014] In terms of fuel properties, these requirements translate into increased thermal conductivity, structural stability, decreased oxidation, and compatibility with any new cladding types that provide benefits to meet the project goals. Several types of non-oxide ceramic fuels are being studied, primarily uranium nitrides and silicides in varying stoichiometries. Metallic fuel designs, fuel additives, and cladding materials are also being studied. Binary uranium nitride (UN) and uranium sesquisilicide (U_3Si_2) have been selected for this research, as they are currently the primary candidates for the ATF program.

1.1. PURPOSE OF RESEARCH

The goals of this research are to:

1.) Investigate and compare the available chemical fabrication processes of selected candidate fuels.

2.) Compare the neutronics performances of the ATF to the current UO_2 fuel in PWR system.

Through the first goal, some options were identified for implementing these designs on an industrial level. Influencing factors may be the need for additional facilities, or advanced research into industrializing certain processes. For the second goal, the reactor performance of selected fuel candidates were simulated with MCNP and compared to that of uranium dioxide. Some neutronic parameters discussed include flux spectra, burnup, temperature coefficients, and moderator to fuel ratio.

1.2. HISTORY OF NUCLEAR FUELS

Throughout the history of nuclear power, there have been numerous designs for fuel based on available technology and the specific reactor application. Many of these have been used in commercial or research applications, others are still in development. The primary criteria for nuclear fuels include power density, fission product retention, structural stability, and chemical compatibility. The two main categories of nuclear fuels are metallic and ceramic forms of either enriched uranium or plutonium.

1.2.1 Metallic. Pure metallic uranium is the most basic form of nuclear fuel, used in early criticality experiments during the Manhattan Project. The world’s first nuclear reactor, Chicago Pile 1, utilized a mixture of metallic and oxide forms of uranium. Most of the first experimental and commercial power reactors also used metallic uranium as fuel including the EBR-I, early MAGNOX reactors, the Russian AM-1, and early CANDU reactors. For thermal power reactors, which mainly used water as coolant, the preferred fuel type became uranium oxides due to the success of the PWR system. For nearly all fast reactors the fuel of choice remained metallic uranium or an alloy. [World Nuclear Association. 2016]

More recently, a startup company called Lightbridge has developed a unique U-Zr alloy fuel assembly design for use in conventional LWR. [Lightbridge, 2016] The Advanced fuels campaign is also studying minor actinide bearing metal alloy fuel. In a breeder or burner type reactor, the use of this type of fuel would be a good method of destroying minor actinides, the primary radiological hazard present in HLW and UNF. [Maloy et al, 2014] Metal or alloy fuels are also being considered for several fast reactor designs being developed by the Gen IV International Forum.

1.2.2. Ceramic. Ceramic compounds of uranium and other fissile and fertile materials have become the standard form of nuclear fuel for commercial power production, medical isotope production, test and research reactors, naval propulsion, and space nuclear applications. The most common is uranium dioxide, but carbide, nitride, and silicide ceramics have also been used for various fast and thermal reactor applications.

Since the construction of the Mark 1 PWR – a prototype engine for the first US nuclear submarine, the *USS Nautilus* – and the successive Shippingport PWR demonstration reactor, this design and similar LWR designs have become the primary systems for commercial power and naval propulsion. [World Nuclear Association, 2016] These reactors have all used uranium dioxide as fuel. UO_2 is the most conventional and widely used nuclear fuel, and has been for nearly the entire history of commercial nuclear power.

However, for high temperature applications, fast reactor designs, space propulsion, and advanced reactor research (past and present), non-oxide ceramics have been preferred over oxide due to enhanced physical properties. While uranium carbide had been considered for several of these applications, it has rarely been used due to its chemical reactivity. [Jones & Crosthwaite, 1973] Uranium nitride has been selected for numerous space nuclear applications including the NASA SP-100 program, among others. [Matthews et al, 1988] Nitride fuel was also used in the Russian BN series of fast reactors. [World Nuclear Association, 2016] Both carbide and nitride have been considered alongside uranium dioxide for TRISO fuel kernels for advanced gas cooled reactors, and as an alternative to metallic fuel for some Gen IV fast reactor designs. [Choi et al, 2006] For smaller non-power reactors at universities, research facilities, and for reactors designed to produce medical isotopes, MTR type fuel elements are the most widely used. This fuel consists of uranium silicide fuel plates layered with plates of aluminum cladding. [Saliba Silva et al, 2008] Regarding the Advanced Fuels Campaign, uranium nitride and silicide ceramics have been selected as candidates for accident tolerant fuels research for light water reactors.

2. ACCIDENT TOLERANT FUEL PROPERTIES

The Advanced Fuels Campaign consists of several areas of research and development including cladding and minor actinide bearing metallic fuel for fast reactors, and accident tolerant fuel and cladding for light water reactors. Only the designs for LWR are considered in this research. Throughout the initial phases of the ATF development program, there have been numerous candidate fuel types proposed by the researchers. These include ceramics in the uranium-nitrogen system, uranium-silicon system, and uranium-boron system. Boron based ceramics are not considered in this research, as there is little research and experimental data available. Borides are also not given as much consideration as the others in the ATF program beyond the initial reports [Brasse, 2014]. These candidates were chosen for use independently or in some form of composite with either another candidate fuel or UO_2. This was done to find the best combination of properties to achieve improved accident tolerance and general performance. Table 2.1 shows the candidate fuels analyzed in this research, and a few key physical properties. Properties of UO_2 and metallic uranium are also shown for comparison.

Figure 2.1 shows the thermal conductivities of the silicon and nitrogen candidate fuels as well as uranium dioxide data as a reference case. In this report, it was concluded that "*U_3Si_2 offers a 17% increase in U- 235 loading and a five-fold increase in thermal conductivity relative to standard UO_2 fuel"* and *"Waterproofed UN would offer up to 35% increase in U-235 loading and 10 times the thermal conductivity of UO_2."* [Braase. 2014] As such, these two fuel types have become the focus of study and experimentation, and are the focus of this thesis.

Table 2.1. Properties of ATF Candidate Materials and UO_2[1]

Property	UO_2	UN	U_3Si_2	U_3Si_5	U
Density(g/cm^3)	10.96	14.31	12.2	9.06	18.95
U-235 Density at 5% enrichment (g/cm^3)	0.48	0.67	0.56	0.38	0.93
Melting Point (°C)	2878	2600	1665	1770	1132

2.1. METAL AND CARBIDE

While having a significant fissile density, there are several significant issues associated with using metallic uranium as fuel. In a reactor environment, metallic uranium will undergo irradiation swelling and anisotropic growth. Both of these phenomena accelerate the migration of fission gases and place additional stress on the fuel elements and cladding materials. [McDonell et al] Additionally, the metallic uranium is easily corroded by water and has a lower melting point relative to ceramics such as uranium dioxide. The improvements in mechanical stability, chemical compatibility with water, and a higher melting point are some of the factors that led to uranium dioxide being chosen as fuel for LWR over metallic uranium. These properties were chosen at the expense of fissile density/power density. This is justified for light water and other thermal reactors, which use a moderator to retain and reflect neutrons from fission, allowing them to operate at a lower flux. However, fast reactors require high power density and flux to sustain fast fission and breeding, and thus require a high fissile density fuel. This design difference is why metallic fuel has been primarily used

---

[1] Data for table from [Puide, 2015]
^{235}U density is a measure of the ^{235}U weight percentage multiplied by compound theoretical density

for most if not all fast reactor applications. Several methods used to overcome the problems of metallic uranium include heat treatments, impurity control, and alloying. [McDonell et al, n.d.]

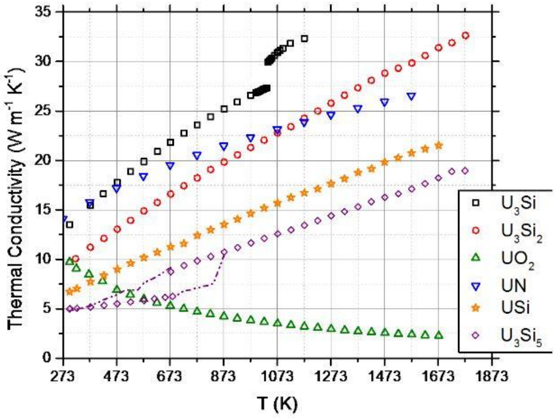

Figure 2.1. Thermal Conductivities of Nuclear Fuels [McClellan, 2014]

Uranium carbides have not been selected for this study, and do not appear frequently in the research related to the Advanced Fuels Campaign. As with uranium nitride, the carbide features high thermal conductivity ceramic with a high uranium density and good physical stability. This combination of properties makes uranium carbide a good compromise between metallic and oxide fuels for fast or thermal systems. However, it is chemically volatile. In air this material will ignite, and readily reacts with water and steam making it difficult to manufacture, transport, and store. These reactions also make this fuel undesirable for use in LWR. [Jones & Croshwaite] As a result, this fuel is often considered but rarely used.

2.2. NITRIDE AND SILICIDE

Uranium nitride possesses many of the attractive qualities of uranium carbide with much improved chemical compatibility. The high thermal conductivity relative to UO_2, relatively high melting point, known fabrication routes, and the existence of performance data have made this fuel type one of the leading candidates for study. [Puide, 2015] However, whenever UN is used in nuclear applications nitrogen enriched in the ^{15}N isotope must be used. Of the two stable nitrogen isotopes, ^{14}N and ^{15}N, nitrogen 14 is 99.636% abundant and has an overall thermal neutron cross section of 11.850 b. The particular reaction of note is an (n, p) reaction with cross section of 1.769 b which yields ^{14}C. The creation of this isotope transforms the fuel into uranium carbide, which is undesirable for the earlier mentioned reasons, as well as the radiological hazards related to ^{14}C. ^{15}N however features an overall thermal cross section of 4.590 b, and features no such detrimental reactions. It is also a stable isotope[2]. The enrichment process adds to the cost of this fuel, but it is necessary to diminish the carbide generation. The most favorable method at this time is laser isotope separation. Centrifugal separation, the current technique for UF_6 enrichment, is not efficient or cost effective for nitrogen given how light the gas is. Chemical and ionic exchange processes are also possible methods for enrichment, but are not considered to be economically feasible routes for industrial scale production, at least in comparison to laser enrichment. [Lahoda & Boylan, 2015]

Another issue with uranium nitride is the tendency and consequences of oxidation when exposed to steam at elevated temperatures. This reaction can take several forms,

---

[2] These cross sections are taken from the JENDL3.2 database, provided by the KAERI Table of Nuclides website

but ultimately produce uranium dioxide and hydrogen gas. Two of these are shown in equations [2.1] and [2.2]. The structural change of this material, as well as the production of ammonia and hydrogen gas within the fuel would be undesirable in normal conditions and accident scenarios. The threshold for these reactions is 300°C, and as such could become a frequent occurrence if not addressed. [Rama Rao et al, 1991] For this reason, for LWR applications or systems where moisture is present, it is advantageous to 'waterproof' uranium nitride by mixing it in a composite with a secondary phase to mitigate this corrosion, similar to alloying of metallic fuels.

$$2UN + 4H_2O \rightarrow 2UO_2 + 2NH_3 + H_2 \qquad [2.1]$$

$$3UN + 2H_2O \rightarrow UO_2 + U_2N_3 + 2H_2 \qquad [2.2]$$

Concerning the silicon fuel types, both selections listed above have different advantages and are both being tested to determine which one is preferred. [McClellan, 2015] In addition to U_3Si_2 and U_3Si_5 uranium, also forms compounds USi and U_3Si among others. Historically, these types of fuel have been made for MTR plate type fuel used in research reactors or medical isotope production reactors. While they have not been used for commercial power production, there is some operational data available. Melting point, thermal conductivity, structural stability, and corrosion resistance were some of the physical properties considered in the initial analysis. Of the existing stoichiometries, the superior properties of U_3Si_2 and U_3Si_5 have made them the preferred candidates in the U-Si system for the ATF program[3]. [Harp, 2015] Both possess exceptional thermal conductivity and are being considered for use in a composite matrix with UN.

---

[3] Research, development, and testing for U_3Si_2 and U_3Si_5 fuel systems is being conducted separately by two different research groups within the ATF Program.

After the initial thermodynamic testing, the following contrast was found between these two compounds: U_3Si_2 possesses higher uranium content and thermal conductivity, while U_3Si_5 shows superior oxidation tolerance and higher melting point. [McClellan, 2015] Figure 2.2 shows images of uranium silicide and uranium dioxide following high temperature steam exposure from the 2014 AFC Ceramic Fuels report. At elevated temperatures, U_3Si_2 disassociates. While U_3Si_5 demonstrates better stability the uranium content is relatively low, lower than even uranium dioxide (see Table 2.1). While these factors reduce the usefulness of these fuels independently, the thermal conductivity and demonstrated oxidation resistance of each makes them attractive in composite mixtures.

Concerning these mixtures, there are two ratios of note that are currently being evaluated. One of the research groups has made a UN-U_3Si_2 composite with 30% U_3Si_2 for irradiation testing. This arrangement seeks to take advantage of the high uranium content of the silicide phase. Another group has proposed UN-U_3Si_5 composites ranging from 5%-30% U_3Si_5. [McClellan, 2015] This research is ongoing and has consisted of several stages of computer modeling, physical testing, and post testing analysis.

Overall, the candidate fuels possess increased thermal conductivity while having lower melting points than UO_2. This is theorized to improve heat removal and allow for lower fuel centerline temperature. [McClellan, 2014] This will decrease the threshold for fuel melting, and will slow the migration of internal fission gases and the subsequent stress generation which may lead to fuel failure. For fuels with increased uranium content the additional fissile density may enable the following: extended cycle length, lower enrichments requirements, power uprates, or reduced core size for similar output.

This may also offset any neutronic penalty incurred with using non zirconium based cladding materials that may have higher cross sections. [McClellan, 2014]

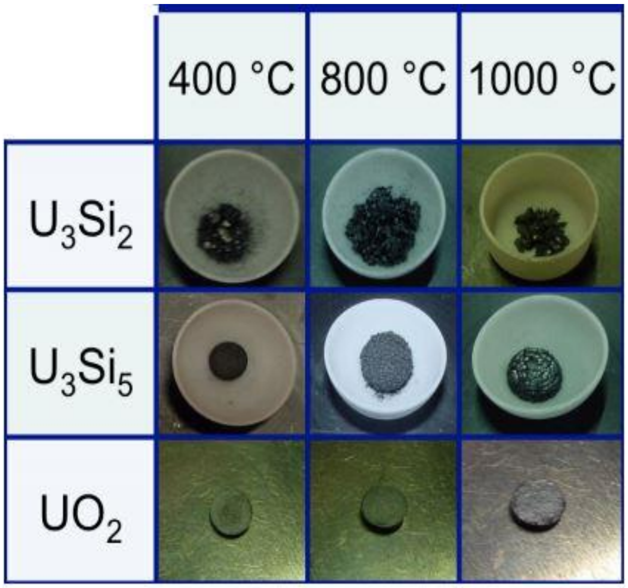

Figure 2.2. U-Si prototypes and UO_2 following exposure to high temperature steam [McClellan, 2014]

2.3. CLADDING PROPERTIES

The advanced fuel cladding prototypes are not the main focus of this research, but their development is parallel and of equal importance to the development of accident tolerant fuels. The main issue with zirconium based cladding is the oxidation and hydrogen production that occurs at high temperatures in steam environments. To mitigate this occurrence, modifications or replacement materials are being investigated. Mechanical durability, heat transfer capability, corrosion resistance, radiation resistance, fuel compatibility, and neutron transparency are all important design criteria for cladding materials. Other cladding types are being developed as a part of the Advanced Fuels Campaign. These design areas include coatings for zirconium cladding, ceramic cladding, and iron based cladding.

As zirconium features many attractive qualities as a cladding material, research has been conducted to determine the effectiveness of coatings on conventional zirconium alloys to provide protection against oxidation in accident scenarios. Stainless steel and a Ti_2AlC compound were considered. The thickness of this coating must be relatively thin to reduce any neutronic penalty. Another of the cladding prototypes developed involves silicon carbide. This is a ceramic material and will exhibit inferior heat transfer capabilities to metal alloys. However, it exhibits superior corrosion and temperature resistances. [Lahoda & Boylan, 2015]

The iron based cladding prototypes include several different oxide dispersion strengthened (ODS) alloys, containing iron, chromium and aluminum. Numerous alloys containing these and other metals are being studied to find the ideal balance of properties for use in a reactor environment. The fact that iron is a significant component of these alloys will result in higher neutron absorption than zirconium cladding. However, the advanced properties and capabilities of these alloys may potentially offset this drawback with the benefits they bring to current and next generation nuclear systems. The combination with higher fissile density fuel may also mitigate this effect. [Braase, 2014]

All of these cladding types are being considered for use with UN/U-Si fuel combinations. [Braase, 2014] It should also be noted that none of these materials are produced on a commercial scale. As with the fuel prototypes, the transition to industrial production must be developed if any of these are to be implemented on a large scale.

3. FABRICATION PROCESS OPTIONS

It is important to note that while the fuels described may have been produced on experimental or bench scales for various research projects or other applications, none are currently produced on an industrial scale like uranium dioxide. However, there still exist numerous methods for synthesis of these materials, some of which are being investigated by the Advanced Fuels Campaign and others that have been developed for various research initiatives and other projects. For the purposes of nuclear fuel, the starting material is often uranium hexafluoride, the form used in enrichment. As such, all steps of stage 1 in Figure 3.1-uranium mining, milling, conversion, and enrichment- will remain unchanged and be considered common to all of the following methods discussed. Additionally, stage 3 of Figure 3.1-pellet manufacture from powdered fuel- will not be discussed in this paper as these steps are common to any powdered nuclear fuel form. For the purpose of this research, only details of stage 2-fuel fabrication up to powdered form- will be discussed. While there are many similarities between the various chemical methods, the feed material for every process is either uranium dioxide or uranium tetrafluoride, reduced from uranium hexafluoride. Methods for production of uranium dioxide and methods for reduction of uranium hexafluoride will be discussed, followed by specific routes of manufacturing uranium nitride and silicide. The considered method for uranium silicide production is the metallothermic reduction processes. Considered methods for uranium nitride synthesis include carbothermic reduction and nitridization (CTR-N), oxidative ammonolysis, and the hydride-nitride method.

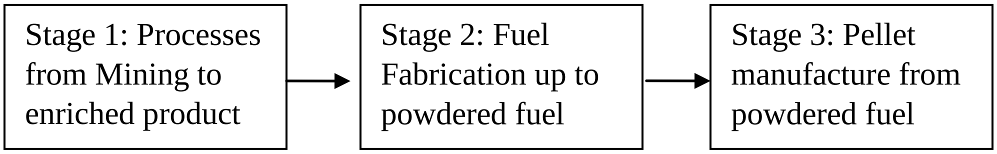

Figure 3.1. Fuel Fabrication Process Flows

3.1. URANIUM DIOXIDE FABRICATION METHODS

Since the first prototype light water reactors were brought online, uranium dioxide has seen the most extensive use in commercial nuclear reactors. The synthesis of this fuel is often linked to the enrichment process. Many of these steps are common to pre enrichment uranium processing as well. Two of the primary uranium dioxide manufacturing methods are the wet ADU process and the integrated dry route.

3.1.1. Wet ADU Method.

In this process, solid uranium hexafluoride is the starting material. This material is vaporized at 13˚ C and then injected into water at 93˚ C to undergo hydrolysis. Both of these reactions occur at atmospheric pressure. [Nuclear Regulatory Commission, 2010] This reaction follows equation [3.1], yielding uranyl fluoride and hydrofluoric acid.

$$UF_6 + 2H_2O \rightarrow UO_2F_2 + 4HF \qquad [3.1]$$

The two products of this reaction are kept in solution and reacted with ammonium hydroxide to yield ammonium diuranate (ADU), ammonium fluoride, and water. Simultaneously, the hydrofluoric acid is neutralized by the ammonium hydroxide to yield additional ammonium fluoride and water. These reactions follow equations [3.2] and [3.3] respectively, and occur at 55˚ C. [Abdelrazek & Zidan, 2002]

$2UO_2F_2 + 6NH_4OH \rightarrow (NH_4)_2U_2O_7 + 4NH_4F + 3H_2O$ [3.2]

$HF + NH_4OH \rightarrow NH_4F + H_2O$ [3.3]

The ammonium diuranate is separated from the solution by centrifuge and then undergoes calcination and reduction in a hydrogen/steam atmosphere to produce uranium dioxide. The calcination is a decomposition of ammonium diuranate to yield uranium trioxide, ammonia, and steam. This reaction occurs at 371˚C. The uranium trioxide is then reduced in hydrogen to yield uranium (III) oxide and steam at temperatures from 500-550˚C. The uranium (III) oxide is reduced in hydrogen to yield uranium dioxide and water/steam at similar temperatures to the previous step. These reactions are described by equations [3.4], [3.5], and [3.6].

$(NH_4)_2U_2O_7 \rightarrow 2UO_3 + 2NH_3 + H_2O$ [3.4]

$3UO_3 + H_2 \rightarrow U_3O_8 + H_2O$ [3.5]

$U_3O_8 + 2H_2 \rightarrow 3UO_2 + 2H_2O$ [3.6]

3.1.2. IDR: Integrated Dry Route. An alternative to the previously described process is the Integrated Dry Route. This process eliminates t aqueous chemistry and reduces number of steps. Uranium hexafluoride is hydrolyzed per equation [3.1] as with the ADU process. The resulting uranyl fluoride is calcined and reduced in hydrogen or steam at around 500˚C to obtain uranium dioxide by equation [3.7]. [Nuclear Regulatory Commission, 2010]

$UO_2F_2 + H_2 \rightarrow UO_2 + 2HF$ [3.7]

3.2. REDUCTION OF URANIUM HEXAFLUORIDE

Uranium tetrafluoride can be produced either from uranium hexafluoride or uranium dioxide. From uranium hexafluoride, chemical reduction following hydrolysis to uranyl fluoride can be achieved with a variety of solvents. Such a reaction using stannous chloride for example follows equation [3.8]. The advantage is a thorough reaction with little impurities and high yield of 98% UF_4 precipitation. [Saliba Silva et al, 2008]

$$UO_2F_2 + SnCl_2 + 4HF \rightarrow UF_4 + SnClF_2 + 2H_2O \qquad [3.8]$$

To achieve uranium tetrafluoride directly, avoiding hydrolysis, uranium hexafluoride can be reduced in hydrogen gas. [Gordon et al, 2006] The preferred reduction occurs in monatomic hydrogen. In reduction with diatomic hydrogen, the reaction is slow and requires high temperatures for an efficient process. However, if the temperature is too high the end products will melt or boil when solid aggregates are preferred. Therefore, the production of monatomic hydrogen is required, via such a process as fluorination, shown in equation [3.9]. A continuous wave chemical laser can be used to achieve this on an industrial level. [Gordon et al, 2006] The reduction occurs in two steps, shown by equations [3.10] and [3.11]. The hydrogen removes a fluorine atom forming hydrofluoric acid twice in succession, first forming uranium pentafluoride, and then again to form uranium tetrafluoride. All three of these reactions occur at 327˚C (600K) [Gordon et al, 2006]

$$H_2 + F \rightarrow HF + H \qquad [3.9]$$

$$UF_6 + H \rightarrow UF_5 + HF \qquad [3.10]$$

$$UF_5 + H \rightarrow UF_4 + HF \qquad [3.11]$$

If uranium dioxide is the desired source material, hydrofluorination can be used to produce uranium tetrafluoride as well. This is a precursor step to enrichment, as uranium is initially extracted as an oxide. The conversion to uranium tetrafluoride is followed by fluorination to produce uranium hexafluoride for enrichment. The same procedure could be used on enriched uranium dioxide as an intermediate step in obtaining metallic uranium. This reversible reaction follows equation [3.12] and occurs over a range of temperatures. [Caplan et al, 1959]

$$UO_2 + HF \rightarrow UF_4 + H_2O \qquad [3.12]$$

3.3. URANIUM SILICIDE PRODUCTION OPTIONS

Uranium silicide has been produced for decades as MTR type fuel for research reactors. [Saliba Silva et al, 2008] However, demand for this type of fuel falls far short of what the demand would be for commercial power reactors so it has only ever been produced on a limited scale. Additionally, limited research into uranium silicon chemistry has left the primary fabrication method of this fuel to be the metallurgical combination of powders. The area of interest then becomes the ideal method for producing metallic uranium. There are several known methods that relate to uranium fluorides and oxides, which meet the Advanced Fuels Campaign requirement that the chosen fabrication routes "*utilize the existing UO_2 manufacturing infrastructure*" so that the fuels may compete economically. [McClellan, 2014] The final step of these processes involves the metallothermic reduction of uranium tetrafluoride. The variation lies in the options for obtaining this reactant. Methods exist starting from uranium dioxide and hexafluoride.

The method for obtaining metallic uranium is known as the Ames process, developed during the Manhattan Project. [Caplan et al, 1959] This is referred to as metallothermic reduction, which a thermite type reaction. An alkali or rare earth metal is burned with uranium tetrafluoride. The volatile reaction of the rare earth metal and halogen species separates UF4 at a high rate, leaving metallic uranium and some form of slag depending on the catalyst. Preferred catalysts include magnesium and calcium (see equations [3.13] and [3.14]). As such, the process can also be called magnesiothermic or calciothermic reduction respectively. The combined reaction temperature and exothermic heat is such that both uranium and slag become molten and can be separated by gravity. Solid slugs of uranium metal can then be separated from the slag once the products solidify. [Caplan et al, 1959]

$$UF_4 + 2Mg \rightarrow U + 2MgF_2 \qquad [3.13]$$

$$UF_4 + 2Ca \rightarrow U + 2CaF_2 \qquad [3.14]$$

In the case of magnesium, the ignition temperature of the reaction is 620˚C, with 49.85 kcal/mol of exothermic heat. The use of calcium could be considered superior in some cases due to a higher exothermic heat of 109.7 kcal/mol. While the efficiency is higher, the handling of calcium increases the cost and difficulty of the process due to its chemical volatility. The use of magnesium is simpler and less costly, which compensates for the decreased efficiency. [Saliba Silva et al, 2008] In either case, uranium tetrafluoride is the required feed material for this reaction.

3.4. URANIUM NITRIDE PRODUCTION OPTIONS

There are several ways that uranium nitride can be produced, dependent or independent of uranium dioxide production methods. Historically, for research applications, uranium nitride has produced from uranium dioxide due to the abundance and ease of access to this material from commercial production. This method is carbothermic reduction and nitridization (CTR-N). However, there have been alternative methods produced attempting to sidestep challenges associated with CTR-N. These are two types of oxidative ammonolysis, featuring ammonia and other nitrogen compounds. Additionally, there are methods for production directly from metallic uranium by nitridation following hydride reduction.

3.4.1. CTR-N: Carbothermic Reduction and Nitridization.

The process analyzed for producing nitride fuel has been used historically for uranium nitride synthesis in various research applications, such as space propulsion reactor and fast reactor projects. [Matthews et al, 1988] The feed material for this process is uranium dioxide. There are two main steps in this process: removal of oxygen with carbon, and removal of carbon with nitrogen. To remove the oxygen, uranium dioxide reacts with carbon to form uranium carbide and carbon monoxide. The carbide then reacts with nitrogen to remove the carbon, forming uranium nitride. This method is not the only possible route of fabricating uranium nitride, but it is the most well-known option available and was the method of choice for the ATF program. Additionally, it is considered to be “the most amenable to near term industrial scale processing.” [McClellan, 2015] The two steps of this process can be arranged and grouped together in various configurations, each way with its own benefits. Part of the ATF research is to identify the ideal setup of reactions [3.15] and [3.16].

$$UO_2 + 3C \rightarrow UC + 2CO \qquad [3.15]$$

$$2UC + 4H_2 + N_2 \rightarrow 2UN + 2CH_4 \qquad [3.16]$$

Equation [3.8] represents step one: oxygen removal; equation [3.16] contains two steps: nitrogen addition and carbon cleanup. [McClellan, 2015] One of the major issues with this process is impurities in the final product (oxygen and carbon). The various routes being developed attempt to minimize the impurities while projecting the ideal industrial scale process. The options for optimizing this method are described in detail in the 2015 Ceramic Fuels Development Annual Highlights, These reactions occur at temperatures of around 1600˚C. [Muromura & Tagawa, 1977] The ultimate advantage to this process is the reality that it is effectively one step in addition to existing uranium dioxide production processes. It is also an amenable method to the use of enriched nitrogen, as it uses gas in a pure form.

3.4.2. Oxidative Ammonolysis. To avoid the high temperatures needed for the CTR-N process, as well as eliminate the concerns of carbon and oxygen impurities, ammonia based methods have been researched to produce uranium nitride. [Yeamans, et al, 2008] Two similar methods will be discussed, one starting with uranium dioxide, and the other with uranium tetrafluoride. When the starting material is uranium dioxide the key reactant is ammonium bifluoride, a common industrial substitute for hydrofluoric acid. This material is milled with uranium dioxide at room temperature and then reacted with ammonia at 800˚C. This yields uranium dinitride, which is then reduced at 700˚C and 1100˚C to binary uranium nitride. This sequence of reactions follows equations [3.17], [3.18], and [3.19]. As with the CTR-N method, this process of ammonolysis is complementary to existing industrial processes for uranium dioxide production.

$$UO_2 + 4NH_4HF_2 \rightarrow (NH_4)_4UF_8 + 2H_2O \qquad [3.17]$$

$$(NH_4)_4UF_8 + 6NH_3 \rightarrow UN_2 + 8NH_4F + H_2 \qquad [3.18]$$

$$4UN_2 \rightarrow 2U_2N_3 + N_2 \rightarrow 4UN + N_2 \qquad [3.19]$$

Alternatively, it is possible to perform a similar reaction while bypassing the production of uranium dioxide altogether. In a similar study, uranium tetrafluoride was reacted with ammonia at 800˚C to produce uranium dinitride. [Chinthanka Silva et al, 2008] The reduction of uranium dinitride follows the same process as the previous method. It is important in this process and in the previous one to keep the reacting atmosphere free of air or oxygen to prevent oxidation impurities. The manufacture of uranium tetrafluoride would be required in addition to the ammonia reaction, which will contribute to the total cost of this particular method.

While these processes may have their advantages, neither involves direct use of nitrogen gas. If the decision is made to use enriched nitrogen in fabrication, the intermediate compounds (ammonium bifluoride and ammonia) must be specially made with enriched nitrogen. This may introduce additional costs and complexity that could negate the advantages of using these methods.

3.4.3. Hydride Nitride: Manufacture from Metallic Uranium. One additional option for producing uranium nitrides involves a direct reaction with uranium metal. This involves two stages of hydriding and nitriding. Metallic uranium is reacted with hydrogen gas at 200-300˚C to form uranium trihydride powder. [Malkki, 2015] The hydride powder is then reduced to metallic uranium powder from 400-600˚C. These steps serve to powderize the metal as an alternative to grinding or milling. If metallic uranium powder can be obtained by a different method, it may possible to skip this step. The metal powder is then heated in nitrogen at 800˚C and then reduced to binary uranium nitride as per equation [3.19]. This process is represented by equations [3.20] and [3.21].

$$2U + 3H_2 \rightarrow 2UH_3 \qquad [3.20]$$

$$4UH_3 + N_2 \rightarrow 2U_2N_3 + 6H_2 \qquad [3.21]$$

A potential issue with the nitriding process may be the agglomeration of the powder, as the reaction produces 507 kJ/mol of exothermic heat. [Malkki, 2015] This may be especially problematic if industrial use of this process is to be considered. The reaction rate or temperature must be carefully controlled to avoid this issue. As with the CTR-N process, this method of uranium nitride features direct use of nitrogen gas which will be amenable to potential use enriched nitrogen. This process may also be seen as an alternative to methods which are additions to existing processes. A significant reduction of steps is possible if nuclear fuel can be fabricated independent of the production of uranium dioxide. This is especially true when considering joint production of uranium nitride and silicide for any composite fuel matrices.

3.5. CHEMICAL PROCESS SUMMARY

While there are many chemical processes available to produce both nitride and silicide nuclear fuel, none of these methods have been implemented on an industrial scale. Some have seen more use than others, but nothing far above lab or bench scale. There are many factors associated with the transition from lab scale to industrial scale that must be addressed. The economics of reactants, equipment, power requirements, and number of steps must all be evaluated to identify the most profitable and feasible method. The question ultimately becomes what is the best utilization of exiting technology and infrastructure to integrate the production of these materials into industrial scale nuclear the fuel production, while minimizing costs in both the short and long terms.

Upon reviewing the described processes, several options seem likely for joint production of uranium nitride and silicide for use in a composite. Flowsheets for these options are available in Appendix A. It is important to note that the potential for any of the above mentioned processes is completely dependent on its large scale economic viability. At any point, further study may reveal one or all of them to be incompatible with industrial production. Until that is determined, all of the options should be equally considered.

To minimize the need for new construction, additions to existing uranium dioxide fabrication facilities could be made. To produce silicide fuel, hydrofluorination of uranium dioxide could be used to produce tetrafluoride, which could then be reduced by the metallothermic method of choice. The metallic uranium could then be combined with silicon to the desired stoichiometry. To produce nitride fuel, the CTR-N process or oxidative ammonolysis process could be used for conversion to nitride. This combination results in the fewest number of new steps required to produce both fuels. However, factoring in the need for nitrogen enrichment suggests that CTR-N may be more feasible, as the ammonium bifluoride must be synthesized with enriched nitrogen. The ultimate decision between enriched nitrogen and enriched ammonia compounds cannot be truly made until a detailed economic comparison is completed.

The previous model is ideal in the short term, as it requires the lowest capital cost. However, it is possible that an eventual replacement of the current infrastructure may reduce long term operating costs if nuclear reactors in the US make exclusive use of the new composite fuel as uranium dioxide is now. This option would eliminate the need for uranium dioxide production post enrichment. Enriched hexafluoride would be reduced in hydrogen to tetrafluoride, and then reduced to metallic uranium with magnesium or calcium. A portion of the metallic uranium would be used in silicide production and the rest would undergo hydride and nitride to produce uranium nitride. Ammonolysis could be substituted here to make uranium nitride if it could be proven economical to make ammonia with enriched nitrogen instead of simply using the gas. While all of the steps with this option would require new construction, the total number of required steps compared to adding on the existing infrastructure may reduce costs in the long term. Chemical process flow sheets depicting the options described are shown in Appendix A.

4. NEUTRONICS SIMULATION

In addition to front end costs, another driving factor behind the development of accident tolerant fuels is that the current levels of operational performance are met or improved upon. In addition to the physical properties described in Section 2, there are various neutronic parameters that need consideration when evaluating a nuclear fuel. These parameters impact safety and reliability as well as economics. Several MCNP models were developed to simulate the use of 70%UN-30%U_3Si_2 composite in LWR. For convenience, this fuel will be further referred to as the composite, as no other composite ratios were simulated in MCNP. Flux profiles, reactivity coefficients, delayed neutron fraction, moderator ratio, and fuel burnup were analyzed. Every simulation was duplicated using uranium dioxide of the same enrichment and configuration to serve as a reference system.

In order to compare neutronic parameters of the composite fuel with existing fuel, and infinite assembly was modeled. A single PWR fuel assembly was constructed in MCNP and boundary conditions were set to create in effect an infinite array of identical assemblies. Visual depictions of this and other models used are included in Appendix B, as well as dimensions, materials, and specifications used for the simulations. Light water coolant, zirconium alloy cladding, and helium fuel/cladding gap filler were used. Some limitations of this model are the lack of control elements, spacer and support materials, and the infinite geometry which does not address reflection or leakage. Additionally, all simulations are based on completely fresh fueled cores and do not address equilibrium cycles.

Another model used simulated a generic PWR based on the core configuration of the Westinghouse AP1000. The operating conditions set for this model are 600 K and 15.5 MPa. Pressure vessel materials, support plates and spacers are not included for simplicity. Several variations of this model were used to evaluate the behavior of accident tolerant fuels compared to the reference fuel, $UO_{2.}$ Control materials were only modeled for shutdown margin and critical boron calculations.

The simulations performed are based on a variation of one of the above mentioned models, depending on what parameter is being evaluated. Infinite lattice models were used to confirm that the region of undermoderation is not impacted significantly by the advanced fuel. The generic PWR model was used to evaluate fuel and moderator temperature coefficients, flux profiles, delayed neutron fraction, burnup, and shutdown margin. For all models, the fuel materials were defined as specified in Table 4.1. Silicon components were based on the natural abundances of silicon isotopes. However, nitrogen content was assumed to be 100% ^{15}N where applicable. U-235 enrichment was assumed to be 3.447% by weight. This is the average enrichment of fuels in a PWR at the beginning of life (based on AP1000 core loading). Additionally, pure oxygen 16, and only uranium isotopes 235 and 238 are considered. The mass densities listed are 94.8% of the theoretical densities listed in Table 2.1.

4.1. MODERATOR TO FUEL RATIOS

The measure of moderator to fuel ratio in a nuclear reactor system is an important factor in analyzing criticality safety. For a transient reactor event, fluctuations in power and therefore temperature may change, causing thermal expansion in the coolant. It is important to know whether this will result in a positive or negative reactivity insertion for a given geometry and material set. To evaluate this, the value of neutron multiplication factor is plotted against the atom ratio of moderator to fuel atoms. The results are shown in Figure 4.1 for UO_2, UN, U_3Si_2, and the composite.

Table 4.1. Fuel Weight Percentages and Densities

Fuel	ρ(g/cc)	U-235	U-238	O-16	N-15	Si-28	Si-29	Si-30
UO2	10.41	0.0304	0.8511	0.1185	-	-	-	-
UN	13.59	0.0324	0.9083	-	0.0593	-	-	-
U3Si2	11.59	0.0319	0.8951	-	-	0.0670	0.0035	0.0024
Comp	12.85	0.0323	0.9043	-	0.0415	0.0201	0.0011	0.0007

When considering the design of a nuclear system, it is advantageous for a system to be undermoderated, where the gradient of the multiplication factor vs. M/F ratio curve is positive. In this case, a decrease in moderator density (resulting from a temperature transient) will cause a negative reactivity insertion. This is a passive design feature from the perspective of criticality safety. Regarding the accident tolerant fuels, the trend is nearly identical to the curve of uranium dioxide, but with a horizontal shift. This shift shows that the ATF curves feature a higher value of k_∞ for the same level of moderation relative to uranium dioxide. This is due to the increased fissile density of the new fuel designs.

The design of current LWR cores requires undermoderation and to have the moderator to fuel ratio well removed from the peak of the curves in Figure 4.1. Thus, if current PWR cores are fueled with the accident tolerant fuels, the core will remain undermoderated. The higher k_∞ values will impact the core excess reactivity. This change in excess reactivity can be overcome using control rods and chemical shim.

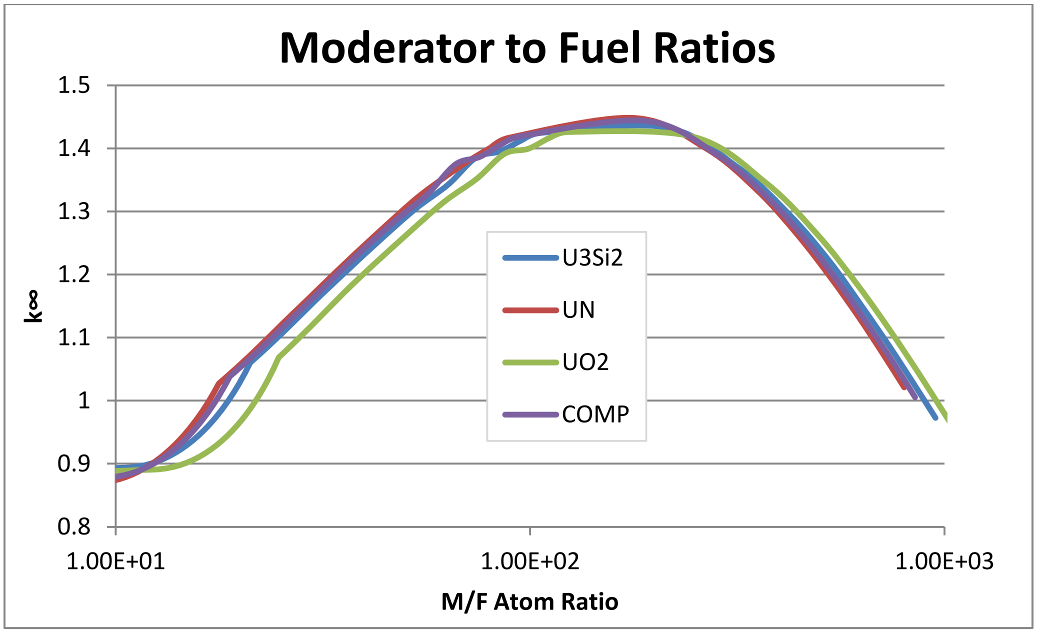

Figure 4.1. Moderator to Fuel Ratios

4.2. ENERGY DEPENDENT FLUX SPECTRA

Lethargy is a measure of neutron moderation, defined as the natural logarithm of a reference energy point divided by the current neutron energy. This normalization shows the degree of moderation in the flux spectrum, which is useful for thermal reactor applications. Figure 4.2 shows the flux per unit lethargy (FPUL) profiles over a range of energies for UO_2, UN, U_3Si_2, and the composite. This data was obtained from the base case infinite assembly simulations used for the moderator to fuel ratio analysis, in which the moderator density is equal to 1.

An important observation is that the trend is identical in shape with regard to energy values. That is to say that the fast and thermal energy peaks are the same as uranium dioxide, but with reduced magnitude. Any shift of the thermal peak would imply a change in the hardness/softness of the flux spectrum in a LWR. This ultimately impacts shielding requirements. The lack of such a shift shows that the use of these fuels will not cause a deviation from standard reactor operating conditions. The significant differences between the spectra are the magnitude of the various thermal peaks. This indicates a variation in the degree of moderation within each fuel, as the geometry and moderating material are the same in each case.

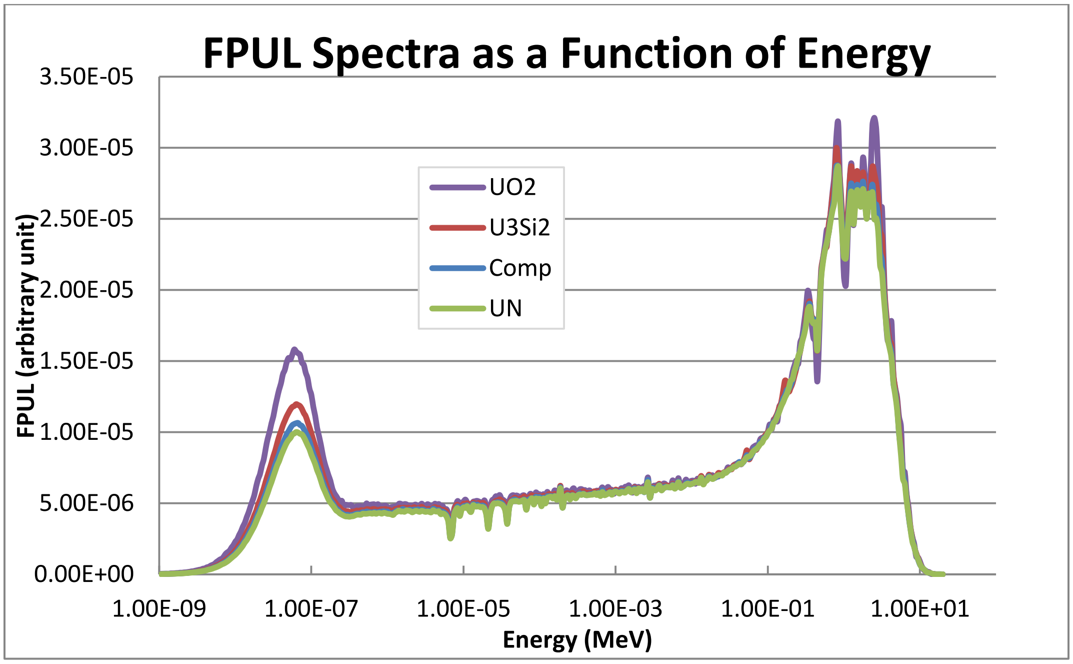

Figure 4.2. Flux Spectra for Infinite Lattice of Various Fuels in PWR Assembly

Each of the non-oxide fuel forms in this analysis possesses higher mass and fissile densities than UO_2. In an identical geometry with the same amount of moderator, the moderator to fuel ratio would be decreased (see Figure 4.1); thus decreasing the degree of moderation in the ATF fueled system relative to the UO_2 reference system.

A good indicator of reduced moderation in a reactor is increased fast fission factor. Hence, fast fission factors were calculated for the infinite lattice model of each fuel type. This result is summarized in Table 4.2. The fast fission factor, ϵ, is calculated using equation [4.1]. For each non oxide fuel, the fast fission factor was higher than that of UO_2; supporting the conclusion that decreased moderator to fuel ratios due to increased fuel density account for the reduced thermal peaks in Figure 4.2.

$$\epsilon = \frac{fast\ fission\ neutrons + thermal\ fission\ neutrons}{thermal\ fission\ neutrons} \qquad [4.1]$$

Table 4.2. Fast Fission Factor Data

Fuel Type	Thermal Value	Fast Value	Fast Fission Factor (ε)
UO_2	7.98995E-04	4.31482E-03	1.185
U_3Si_2	1.39695E-03	6.44699E-03	1.217
Composite	1.18733E-03	4.93567E-03	1.241
UN	1.10666E-03	4.35964E-03	1.254

For this analysis and the analysis of moderator to fuel ratios, the behavior of UN and U_3Si_2 were only included as an additional reference for analyzing the properties of the composite using the infinite lattice model. As described in Section 2, the focus is to use a composite fuel of nitride and silicide in LWR. Furthermore, the neutronic characteristics of the composite fuel fall between those of the nitride and silicide. As such, only UO_2 and the composite are considered from this point forward.

4.3. TEMPERATURE COEFFICIENTS

Another important criticality safety parameter is the temperature reactivity coefficient of fuel and moderator materials. A change in material temperature can result in a positive or negative reactivity insertion. For fuel and moderator/coolant materials is it important that this quantity be negative so that if reactor cooling is lost, power will not increase. Using the PWR core model, fuel and moderator temperature coefficients were calculated for composite and uranium dioxide fueled cores. For each fuel, the simulation was run three times. The first case (C_0) was a base line simulation, with the MCNP material cross section libraries set for the 300 K temperature state. For the second case (C_1), the temperature state of the fuel, gap, and cladding materials was changed to a 600 K temperature state, while the water in the system was left at the 300 K state. The third case (C_2) defined all material cross sections at the 600 K temperature state. The temperature modifications were necessary to isolate fuel and moderator as separate variables for the analysis.

Reactivity change was computed from the values of average neutron multiplication factor (k_{eff}). Equations [4.2] and [4.3] are used to calculate reactivity change and the temperature coefficient. Between the first and second cases, only the fuel materials changed temperature, isolating the effect of the fuel temperature change on reactivity. The k_{eff} values from these two simulations were used to compute the fuel temperature coefficient. A simplifying assumption for this analysis is that the density change of the fuel would be negligible for a temperature increase of 300 K. Similarly, between Case 2 and Case 3, the only temperature change was that of the water. In this case the density of water was changed according to the temperature and pressure states. All of the input parameters and results are shown in Table 4.3. While there are differences in the values for the different fuels, both coefficients are negative and on the same order of magnitude indicating comparable reactivity response to temperature. It should be noted that this analysis is the only time the temperature states of this MNCP model were changed from the default setting. All other simulations discussed with this model use the 600 K state (the reference case C_2).

$$\Delta\rho = \frac{k_2 - k_1}{k_2 k_1} \quad [4.2]$$

$$\alpha = \frac{\Delta\rho}{\Delta T} \quad [4.3]$$

Table 4.3. Fuel and Moderator Temperature Coefficient Data

Case	Fuel Temp (K)	Coolant Temp (K)	Water Density (g/cc)	k_{eff}	Reactivity (Δk/k)	Re. Co. α, fuel	Re. Co. α, moderator
Comp							
C_0	300	300	1.005	1.42190	-	-	-
C_1	600	300	1.005	1.40955	-0.00616	-2.05398E-05	-
C_2	600	600	0.649	1.32797	-0.04358	-	-0.00015
UO2							
C_0	300	300	1.005	1.42641	-	-	-
C_1	600	300	1.005	1.41492	-0.00569	-1.89768E-05	-
C_2	600	600	0.649	1.34779	-0.03520	-	-0.00012

4.4. DELAYED NEUTRON FRACTION

The value of delayed neutron fraction (β) is a measure of delayed to total neutrons in a reactor system. This fraction can be seen as the minimum value of a positive reactivity insertion that would cause the reactor to become prompt critical. Safety limits on reactivity insertions are set based on this value. To measure this quantity, the prompt multiplication factor (k_{prompt}) is required as well as the overall multiplication factor (k_{eff}). MCNP allows the user to use total neutrons or only prompt neutrons when calculating multiplication factor. Use of only prompt neutrons will give the prompt multiplication factor (k_{prompt}) Equation [4.4] can be used to calculate delayed neutron fraction. For the UO_2 core the computed value of β was 0.007326; the value for the composite core was 0.007103. These values are comparable, indicating no significant change in this parameter from using the prototype fuel.

$$\beta = 1 - \frac{k_p}{k} \qquad [4.4]$$

4.5. RADIAL AND AXIAL FLUX PROFILES

The power distribution profiles of the two core layouts will give projections of temperature and flux levels throughout the core, as well as the expected peaking factors for these and other parameters. This information is useful for safety analysis, optimization, and maintenance. Using MCNP6 mesh tallies of the PWR model for UO_2 and composite fuel, normalized flux profiles were obtained for radial and axial dimensions. A mesh equivalent to a unit fuel element lattice was used for the flux profiles. Figures 4.3-4.5 show the radial profiles of the UO_2 and composite cores in 3D and xy-plane 2D views, as well as a comparison of the 1D axial flux profiles. The peaking factors, calculated as maximum over average flux, are 3.00 for the composite and 2.73 for UO_2. The overall flux magnitude from the UO_2 fueled core is higher than that of the composite ATF core. This is due to the lower fissile content in the UO_2 core. The increased peaking factor in the composite fueled core may necessitate improved flux flattening strategies.

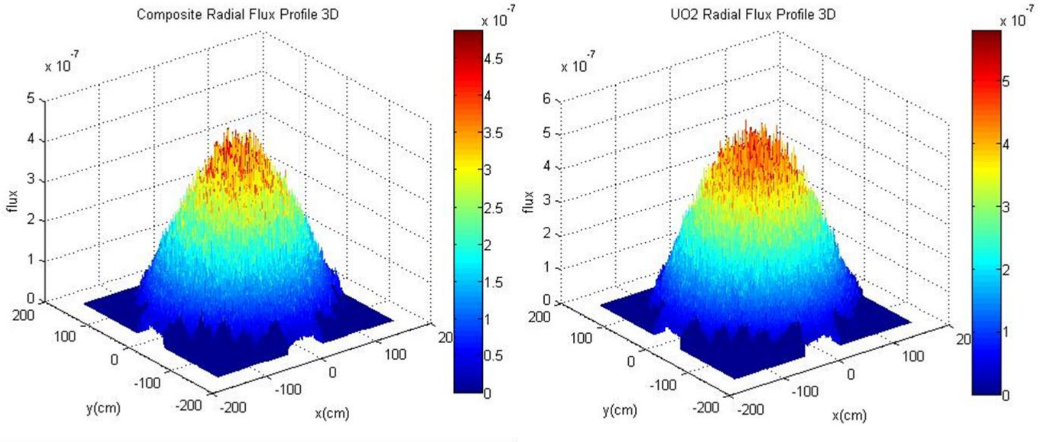

Figure 4.3. Composite and UO_2 3D Flux Profile

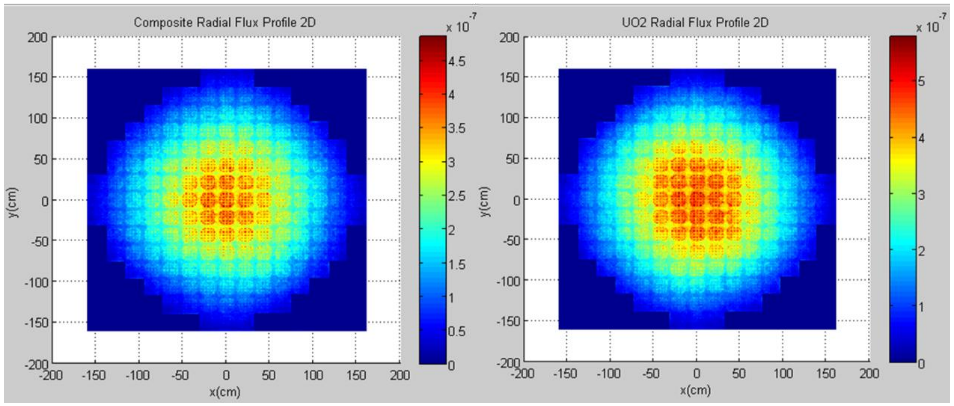

Figure 4.4. Composite and UO_2 2D x/y Plane Flux Profile

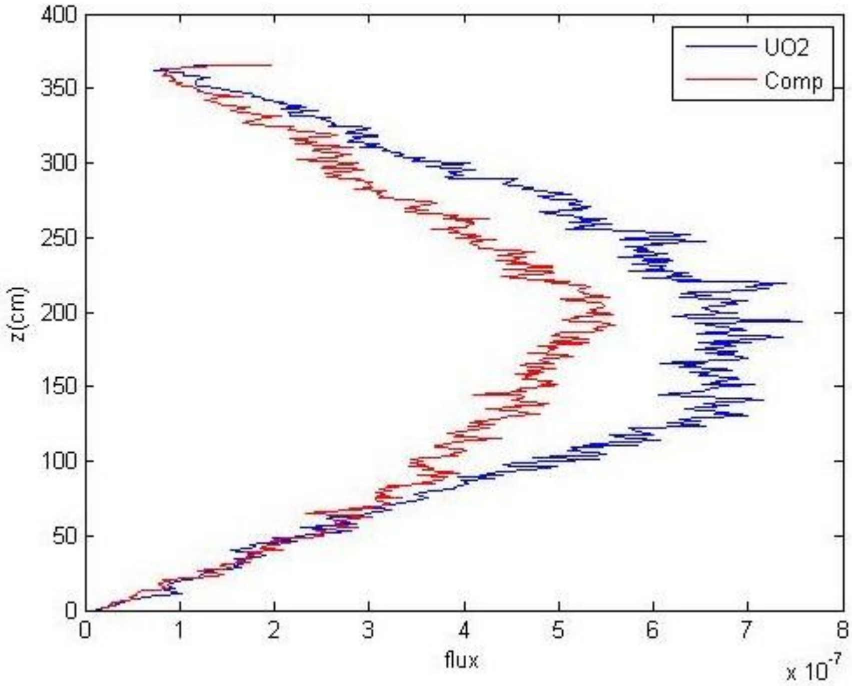

Figure 4.5. Axial Flux Profiles

4.6. BURNUP ANALYSIS

An important metric for evaluating the resource utilization potential of a nuclear fuel material is projecting and evaluating the consumption and production of fissile material. This analysis is important in optimizing reactor cycle lengths and fuel loading options. For the PWR MCNP model, depletion simulations were performed for the composite and UO_2 fuels. The parameters for the simulations include 16 time steps of 100 days for a total of 1500 days (50 months) at a power of 3411 MWt with a 91% power fraction. The same fuel is used for the entire 1500 days with no simulated outages or refueling. The transition of multiplication factor with time is shown in Figure 4.6. Although, the fissile content of the composite ATF fueled core is higher than the UO_2 reference core, the UO_2 core has the higher excess reactivity at the beginning of life

(BOL) of both configurations. The BOL multiplication factors for the UO_2 core and composite core are 1.34 and 1.32 respectively[4]. Over time, the UO_2 core's multiplication factor decreases at a higher rate than that of the composite core. This is expected due to the increased fissile loading of the composite ATF fueled core. The UO_2 reference core became subcritical after 800 days while the composite ATF core was extended till 1000 days before subcriticality. This indicates a more rapid depletion of fissile materials in UO_2 reference core compared with the composite ATF core. At the onset of subcriticality, the UO_2 fueled core attained a burn-up of 27.5 GWd/MTIHM. The burn-up at onset of subcriticality for the composite ATF fueled core is 26.3 GWd/MTIHM. Thus, the composite fuel extended the cycle life by 200 days, but led to a burn-up penalty of 1.2 GWd/MTIHM.

The dynamics of multiplication factor over the core life and the resultant burn-up is driven by the fissile contents of the core configuration. A total fissile fraction at any time is defined as the ratio of the sum of ^{235}U and ^{239}Pu masses to the initial mass of ^{235}U loaded in the core. This definition is conservative since it neglects the ^{241}Pu content, which is also a fissile nuclide. The ^{241}Pu generated in LWR is a small fraction of ^{239}Pu content.

Furthermore, the ^{241}Pu content is expected to reduce significantly during post-discharge cooling time for the used nuclear fuels. The half-life of ^{241}Pu is 14.4 years, which implies that 21.4% of the ^{241}Pu would have decayed in 5 year cooling period. The ^{241}Pu loss is 61.8% for a 20 year cooling period. For these reasons, only the ^{235}U and ^{239}Pu are captured in the fissile fraction.

---

[4] Averages computed over 200 cycles in MCNP6
Composite BOL multiplication factor standard deviation is 0.00034
Oxide BOL multiplication factor standard deviation is 0.00030

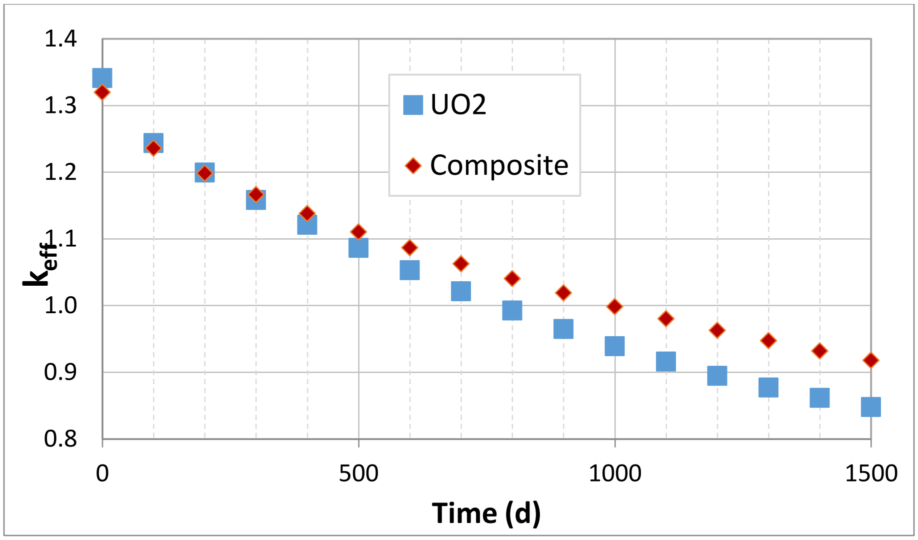

Figure 4.6. Multiplication Factor vs. Time in UO_2 and Composite Fueled Cores

Figure 4.7 shows the change in fissile content as a fraction of initial uranium loading. The fuels are deemed discharged at the point where the respective cores become subcritical. The total fissile fraction from UO_2 fuel at discharge is 0.431 while that of the composite fuel is 0.497. The ^{235}U fissile fraction at discharge is smaller for the UO_2 core. At discharge, the fissile fraction of ^{239}Pu generated in the UO_2 and composite cores are 0.185 and 0.208 respectively (see Fig. 4.7). These are indications that the UO_2 core has higher fuel utilization that the composite fuel in an identical configuration. With core configuration optimization specific to the composite ATF fueled core, a composite core could sustain a longer cycle to produce the level of burnup attained in the UO2 core or better. Alternatively, a reduced initial fissile loading (i.e. lower enrichment) could potentially produce a comparable rate of fuel depletion over time. An extended cycle length or reduced levels of enrichment are both possibilities that translate to potential fuel cycle benefits for nuclear power operators.

4.7. SHUTDOWN MARGIN & CRITICAL BORON CONCENTRATION

One method of ensuring appropriate reactivity control in LWR systems is the presence of soluble boron dissolved in the coolant in the form of boric acid. The concentration of boric acid can be precisely controlled on a scale of parts per million it allows for uniform reactivity insertions unattainable by control rods. The concentration required to make the core critical on soluble boron alone is the critical boron concentration. Adding additional boron to the system above the critical concentration provides an alternative means to shut down the reactor if the control rod mechanisms malfunction.

For the UO_2 and composite PWR core models, the critical boron concentrations were calculated by adding boron in varying amounts to the water in the system. The variant of the models used for this analysis did not feature control assemblies. The simulations were run several times for a series of varying boron concentrations in ppm to determine the value of k. The theoretical critical concentration was interpolated from this data, as well as the smallest possible concentration that would make the system subcritical. Only concentrations of pure boron 10 are added, rather than boric acid (H_3BO_3), the form of soluble boron used in nuclear reactors. Initial simulations were performed at concentrations of 500, 1000, 1500, and 2000 ppm.

Figure 4.8 shows the transition in multiplication factor (k_{eff}) with boron (^{10}B) concentration. The trend was determined with second degree polynomial. The trend was used to determine the critical boron concentration for both UO_2 core and Composite fuel core. The critical ^{10}B concentrations are 1282 ppm and 1557 ppm for the UO_2 core and Composite fuel core respectively. The higher value of critical boron for the Composite fuel core is indicative of the decreased thermalization in the core. ^{10}B has excellent thermal neutron absorption cross section. As neutron energy increases, ^{10}B neutron absorption effectiveness drops. As discussed in Section 4.2, there is decreased thermalization in the Composite fuel system. Thus more ^{10}B atoms are required to compensate for the drop in absorption effectiveness of boron content.

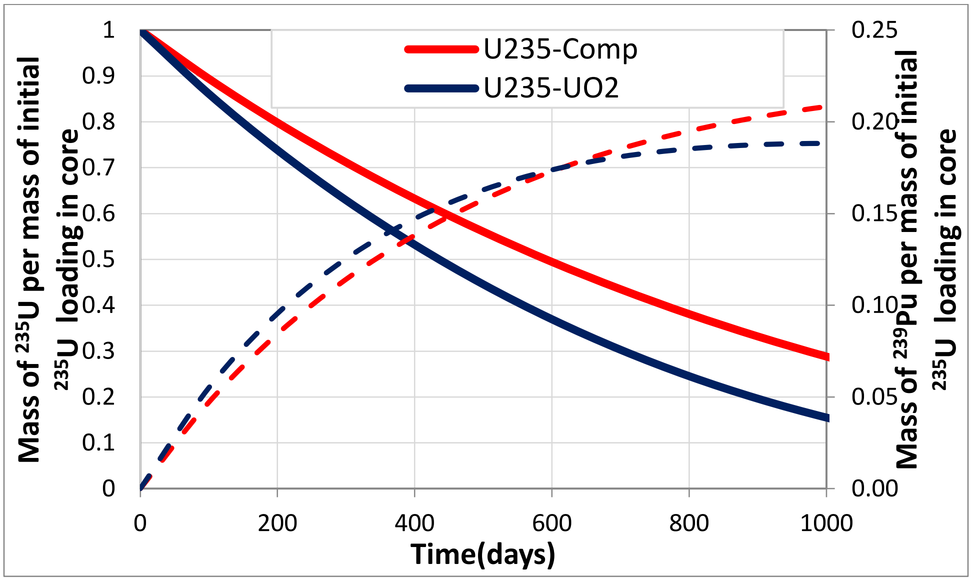

Figure 4.7. Fissile Fraction in the Core over 1500 Days of Operation

An important criticality safety parameter in nuclear reactors is shutdown margin. Shutdown margin is defined as the amount by which the reactor core would be subcritical at shutdown if all control rods except the one with highest worth are inserted into the core while maintaining critical boron level as well as the levels of other dispersed neutron absorbers (like xenon).

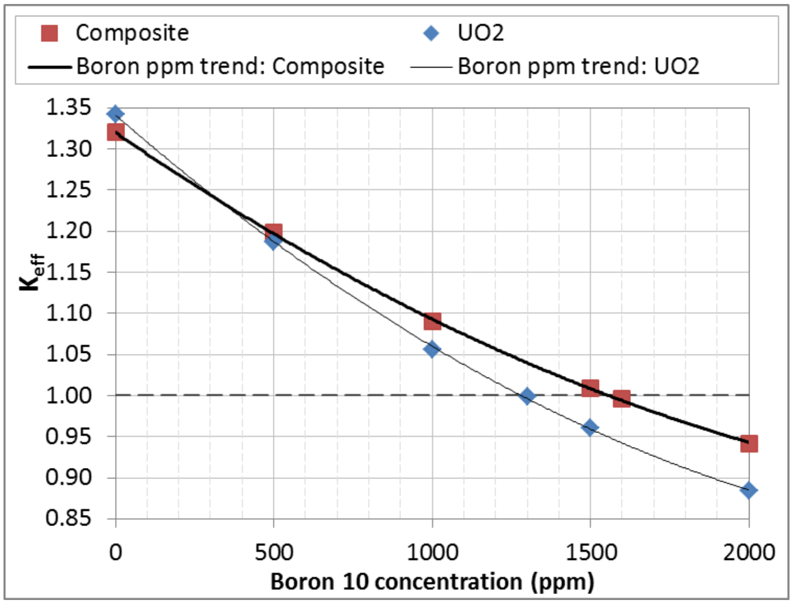

Figure 4.8. Multiplication Factor vs. ^{10}B Concentration in UO_2 and Composite Cores

For this analysis, two types of control assemblies were added to the standard PWR model. These are the Reactivity Control Cluster Assembly (RCCA) and the Gray Rod Cluster Assembly (GRCA) used in various Westinghouse reactor designs including the AP1000. [Franceschini et al, 2015] These two assemblies are similar in design: a cluster of absorbing rods in cladding tubes that inserts into a standard fuel assembly. The dimensions and cladding material is the same for these two designs (see Table 4.4). [Franceschini et al, 2015] The difference between the RCCA (also called a black rod assembly) and the gray rod assembly is the composition of the rods themselves. The black assembly rods are made of 24 rodlets of 80-15-5 AIC with SS 304 cladding. The gray assembly rods are made of 24 alternating rodlets of AIC and SS 304 in the cladding tube, similar to how fuel pellets are stacked in fuel rods. Specific dimensions of the black and gray assemblies are listed in Table 4.4. Total rod height refers to the active length of the assembly- the length that is in contact with the fuel. Black and gray assemblies were evenly distributed in the core lattice, including 63 black and 15 gray per the reactor design. [Franceschini et al, 2015]

The generic PWR model was modified to include gray and black control assemblies accordingly. The configuration is shown in Figure 4.9. [Nuclear Regulatory Commission, 2012] In Figure 4.9, the gray assemblies are in spaces shaded gray, black assemblies making up the rest. The definition of shutdown margin includes a safety factor disregarding the highest worth rod or assembly in a system. For that purpose, the central black assembly (position 8H) was removed for these simulations, replaced by a normal fuel assembly cell.

The simulations were performed, and values of k_{eff} were obtained for each model. Since shutdown margin (SDM) by definition is the margin by which a reactor is subcritical at shutdown, a gross SDM was defined as the control rod worth for a core made critical solely by boron dissolution. In order to determine the gross SDM, the base case C_0 (see Table 4.3) was modified with the control rod insertion scheme. It should be noted that the k_{eff} of the core with control rod but without burnable poison/chemical shim is greater than unity. This is because the negative reactivity inserted by control rod rods is not sufficient to overcome the excess reactivity built into a fresh PWR core. The change in k_{eff} induce by the control rod insertion is indicative of the reactivity worth of the control rods. Equation 4.2 was used to compute the reactivity change between the cores with and without control elements. The results are shown in Table 4.5.

Table 4.4. Control Rod Cluster Dimensions

Dimension	Measurement(cm)
Rod height(total)	360
Rodlet height(gray assembly only)	15
Rod/Rodlet Diameter	0.866
Clad tube outer diameter	0.967
Clad tube thickness	0.04699

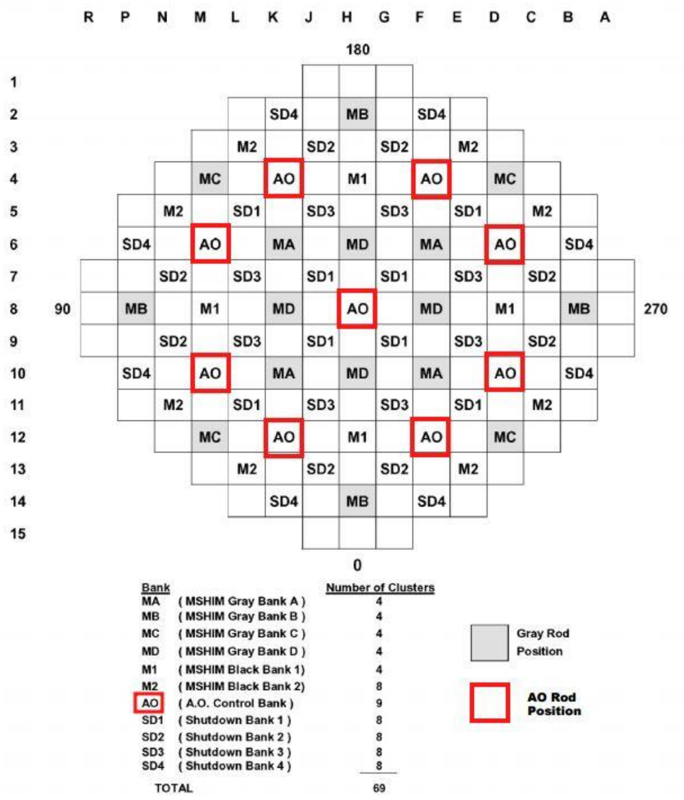

	R	P	N	M	L	K	J	H	G	F	E	D	C	B	A
1															
2						SD4		MB		SD4					
3					M2		SD2		SD2		M2				
4				MC		AO		M1		AO		MC			
5			M2		SD1		SD3		SD3		SD1		M2		
6		SD4		AO		MA		MD		MA		AO		SD4	
7			SD2		SD3		SD1		SD1		SD3		SD2		
8		MB		M1		MD		AO		MD		M1		MB	
9			SD2		SD3		SD1		SD1		SD3		SD2		
10		SD4		AO		MA		MD		MA		AO		SD4	
11			M2		SD1		SD3		SD3		SD1		M2		
12				MC		AO		M1		AO		MC			
13					M2		SD2		SD2		M2				
14						SD4		MB		SD4					
15															

Bank		Number of Clusters
MA	(MSHIM Gray Bank A)	4
MB	(MSHIM Gray Bank B)	4
MC	(MSHIM Gray Bank C)	4
MD	(MSHIM Gray Bank D)	4
M1	(MSHIM Black Bank 1)	4
M2	(MSHIM Black Bank 2)	8
AO	(A.O. Control Bank)	9
SD1	(Shutdown Bank 1)	8
SD2	(Shutdown Bank 2)	8
SD3	(Shutdown Bank 3)	8
SD4	(Shutdown Bank 4)	8
TOTAL		69

Figure 4.9. AP1000 Control Assembly Layout
[Nuclear Regulatory Commission, 2012]

The gross SDM are 0.10943 Δk/k and 0.09713 Δk/k for the UO_2 and Composite fueled cores respectively. These values are within 0.0123 Δk/k of each other; thus comparable. It should be noted the gross SDM values are adequate to accommodate neglected sources of positive reactivity insertion during shutdown transient. These sources include power defect, doppler/temperature reinsertion of reactivity, uncertainties due to control rod depletion and insertion, uncertainties due to void effects, uncertainties due to xenon transient/perturbation, Doppler uncertainties, and moderator uncertainties. The aggregate effect of these sources practically cannot overcome the gross SDM introduced by the control rod insertion.

Table 4.5. Shutdown Margin

Composite		
Case	**k value**	**ρ**
Base	1.31995	0.24240
Base plus Control Rod (CR) insertion	1.16995	0.14526
Base plus Critical Boron and CR	0.90615	-0.10357
Gross SDM (CR Worth)		-0.09713
UO2		
Case	**k value**	**ρ**
Base	1.34162	0.25463
Base plus Control Rod (CR) insertion	1.16987	0.14520
Base plus Critical Boron and CR	0.89574	-0.11640
Gross SDM (CR Worth)		-0.10943

4.8. NEUTRONICS RESULTS SUMMARY

For all of the neutronic parameters considered, the composite fuel showed comparable performance to UO_2 in an identical core configuration. The moderator to fuel ratios showed both fuels to be undermoderated in the same configuration. There was a slight shift with the composite curve, indicating higher excess reactivity than a UO_2 core. The infinite assembly flux energy profile and core flux profiles also showed similar trends. However, the magnitude of the peaks for the non-oxide fuels was lower than that of UO_2. This is due to the reduction in the degree of thermalization within the fuel, a consequence of the reduced moderator to fuel ratio resulting from increased densities of the non-oxide fuels. The corresponding increase in fast fission factors of the non-oxide fuel models supports this conclusion. Temperature coefficients for fuel and moderator and delayed neutron fractions of both cores were within 3.1%, 6.5% and 3.0% of each other respectively. This indicates that the Composite fueled system no significant change in criticality safety parameters from those of the reference UO_2 reactor system. The power peaking factors of the composite and oxide systems were 3.00 and 2.73 respectively

The burnup analysis showed a decreased rate of ^{235}U consumption for the composite core compared to the UO_2 core (11% of initial ^{235}U to 2.9% respectively). Additionally, the composite core demonstrates increased plutonium production over the same length of time and power level as a UO_2 fueled core (22% to 18% respectively). These results suggest the possibility of a cycle length extension, enrichment reduction, or other fuel cycle improvements as potential benefits of using composite fuel. Regarding reactivity control, the estimated critical boron concentration for a composite fueled core (1557 ppm) is higher than that of a similar UO_2 fueled core (1282 ppm) by 275 ppm of ^{10}B. Using the configuration of black and gray control rod assemblies designed for the Westinghouse AP1000, the shutdown margins of both cores were similar within 0.0123 $\Delta k/k$. The gross SDM of the composite fuel core was 11.24% lower than that of the UO_2 core. Despite the decrease, the composite SDM is still adequate for the purposes of safe shutdown.

These analyses indicate that the use of composite fuel in existing core configurations will not require any significant modifications to comply with current PWR neutronics standards, and may enable fuel cycle improvements. Further analysis should include extended equilibrium cycle burn runs to further evaluate the burnup performance and fission product production of the composite fuel. More detailed models featuring structural systems, instrumentation, and burnable absorbers unique to various reactor designs should be used for a reactor-specific approach to this analysis.

5. CONCLUSIONS

As a method of improving the safety of LWR, and nuclear reactors in general, the fuel can be redesigned to resist common and unusual accidents. Such improvement would prevent fuel damage, system failure, and ultimately excessive radiation exposure. Several types of accident tolerant fuels have been developed, the most promising of which being a composite of uranium nitride and silicide ceramics. Improvements in physical properties over uranium dioxide include higher thermal conductivity and increased fissile density. Thermodynamic performance, irradiation stability, corrosion resistance, and other performance properties of these prototypes are being evaluated to determine if these accident tolerant fuels may be an acceptable substitute for uranium dioxide to achieve a higher level of safety and robustness in nuclear systems.

All physical properties and performance aside, such fuels will only be viable if the means of fabrication on an industrial level exists and is economical compared to the existing infrastructure. A variety of chemical methods exist to fabricate uranium nitride and silicide featuring starting materials common to the current UO_2 infrastructure; either UO_2 or UF_6 can be used. The process options for nitride production include, but are not limited to carbothermic reduction, ammonolysis, and a combination of hydridization and nitridization. For silicide production, metallic uranium must be produced. The most well-known method for this is metallothermic reduction of UF_4. UF_4 can be obtained several ways, through direct reduction of UF_6 or from UO_2 via hydrofluorination.

For a combined fabrication infrastructure to produce both types in a composite, there are several options. One option requires a minimal amount of new construction.

Existing fuel fabrication infrastructures are primarily for oxide fuels. The UO_2 from these infrastructures could be used as the starting material for the nitride and silicide. This will likely cost less in the short term and is amenable to joint production of UO_2 and composite fuels. Another option requires additional new construction, but in the long term allows for production of composite fuel with a significant reduction in the number of steps. This is possible as the production of UO_2 is bypassed altogether.

For separate and more efficient production of composite fuel, or if UO_2 is ever phased out as a nuclear fuel, this option could be considered. Ultimately, the commercial viability of the composite fuel is subject to the economic feasibility of each chemical method on an industrial scale, which will be a significant factor in the commercial deployment of these fuels.

Another consideration with new nuclear fuel in addition to physical performance and production economics is the in core nuclear performance of the fuel relative to UO_2. Various MCNP simulations were performed with the composite fuel and uranium dioxide as the reference. The overall neutronic behavior and characteristics are comparable between both fuel types. As such, no significant modifications to reactor licensing or operating procedures are foreseen. However, the simulations did show higher fissile fractions in the composite assemblies than the UO_2 fuel assemblies at discharge. This has several implications. An optimization of the composite fueled core and/or reduction in the initial fissile loading of the composite core may lead to improved fuel utilization/economy. These factors suggest the possibility of improved fuel economy when using composite fuel, which may enable fuel cycle improvements in addition to the potential improvements in safety.

APPENDIX A

CHEMICAL PROCESS FLOW SHEETS

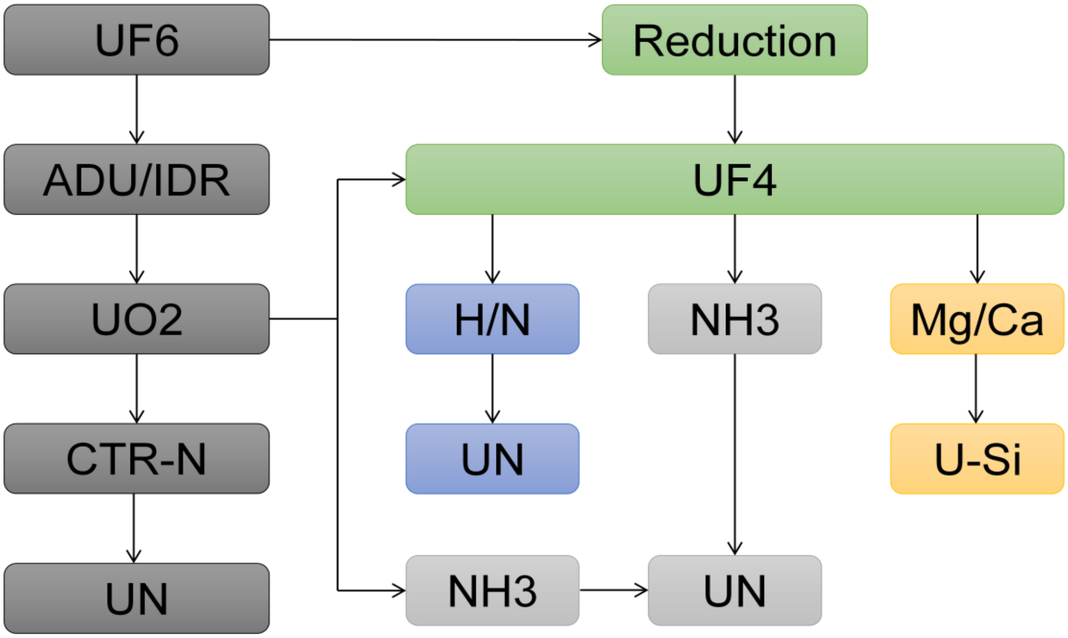

Figure A1. Overall Chemical Process Flows for Accident Tolerant Fuels

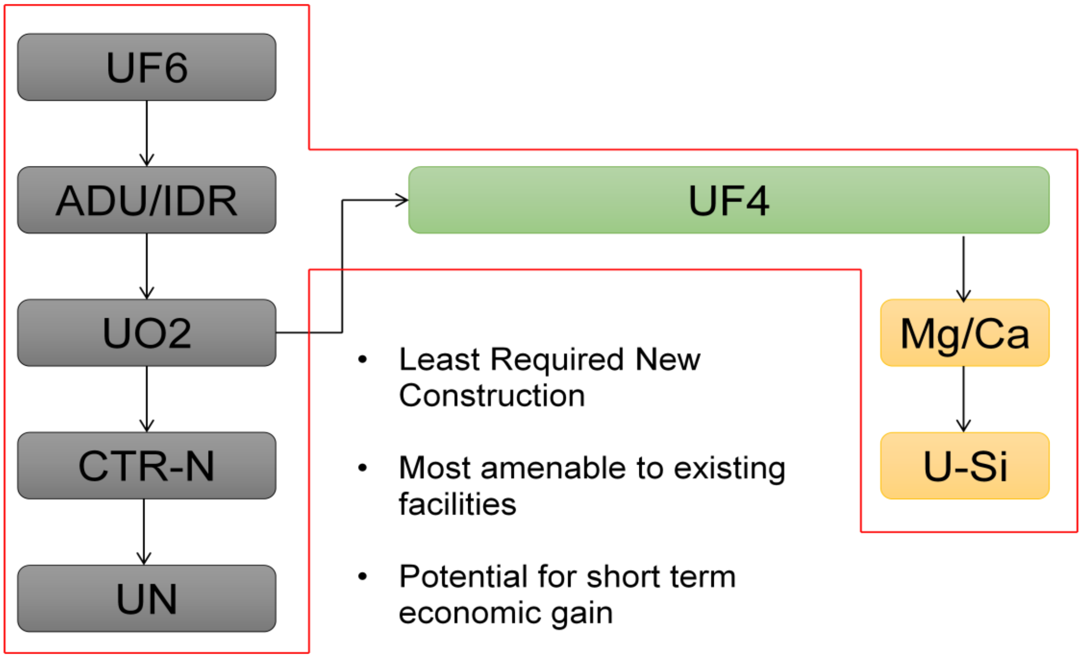

- Least Required New Construction
- Most amenable to existing facilities
- Potential for short term economic gain

Figure A2. Option 1 Process Flow: CTRN to UN; Hydrofluorination, UF_4 Reduction to Silicide

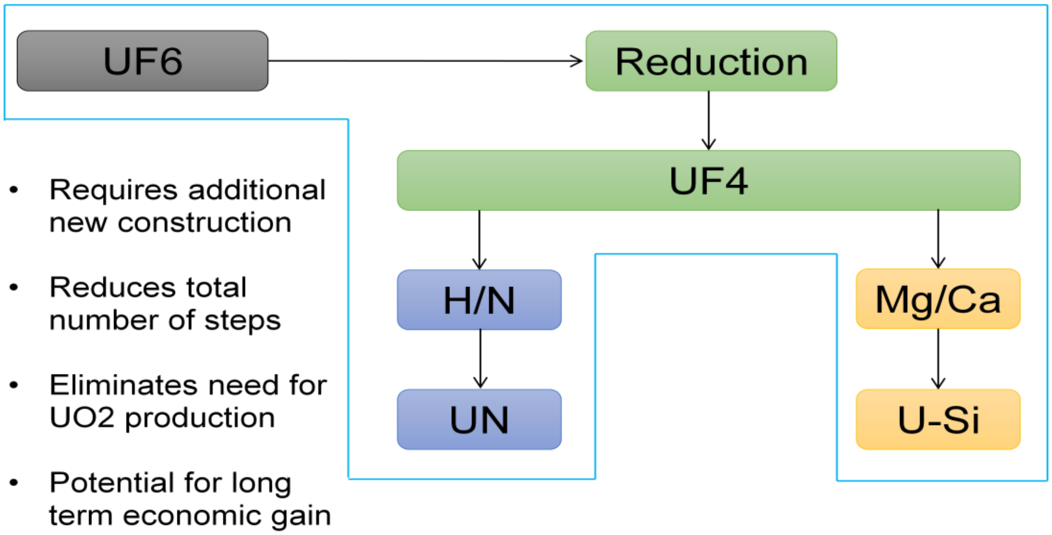

- Requires additional new construction
- Reduces total number of steps
- Eliminates need for UO2 production
- Potential for long term economic gain

Figure A3. Option 2 Process Flow: UF_6 Reduction to UF_4, Hydride/Nitride Reduction to UN; UF_4 Reduction to Silicide

APPENDIX B

MCNP MODELS AND DATA

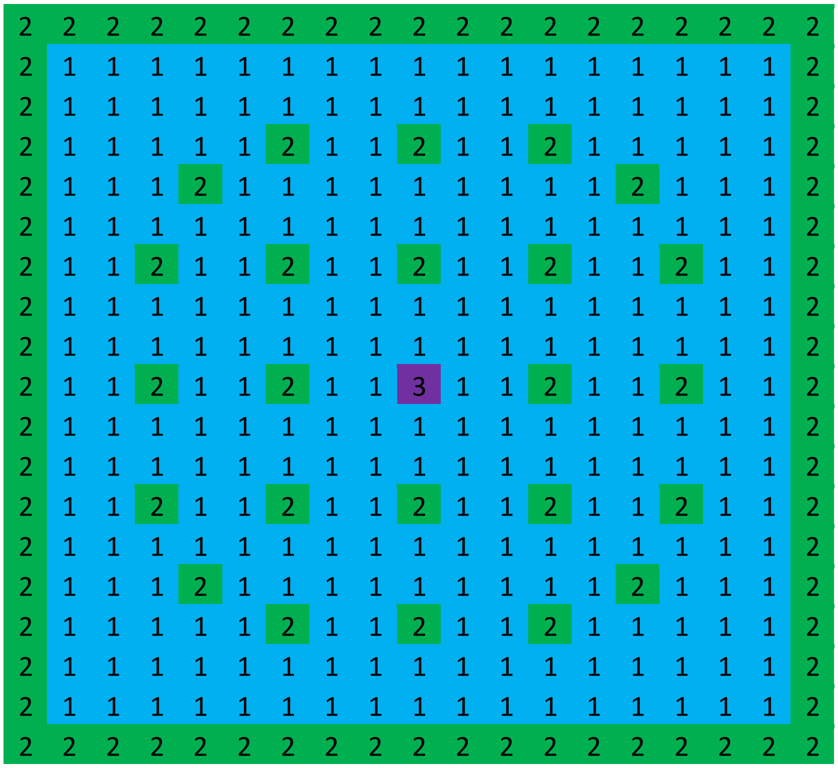

2	2	2	2	2	2	2	2	2	2	2	2	2	2	2	2	2	2	2
2	1	1	1	1	1	1	1	1	1	1	1	1	1	1	1	1	1	2
2	1	1	1	1	1	1	1	1	1	1	1	1	1	1	1	1	1	2
2	1	1	1	1	1	2	1	1	2	1	1	2	1	1	1	1	1	2
2	1	1	1	2	1	1	1	1	1	1	1	1	1	2	1	1	1	2
2	1	1	1	1	1	1	1	1	1	1	1	1	1	1	1	1	1	2
2	1	1	2	1	1	2	1	1	2	1	1	2	1	1	2	1	1	2
2	1	1	1	1	1	1	1	1	1	1	1	1	1	1	1	1	1	2
2	1	1	1	1	1	1	1	1	1	1	1	1	1	1	1	1	1	2
2	1	1	2	1	1	2	1	1	3	1	1	2	1	1	2	1	1	2
2	1	1	1	1	1	1	1	1	1	1	1	1	1	1	1	1	1	2
2	1	1	1	1	1	1	1	1	1	1	1	1	1	1	1	1	1	2
2	1	1	2	1	1	2	1	1	2	1	1	2	1	1	2	1	1	2
2	1	1	1	1	1	1	1	1	1	1	1	1	1	1	1	1	1	2
2	1	1	1	2	1	1	1	1	1	1	1	1	1	2	1	1	1	2
2	1	1	1	1	1	2	1	1	2	1	1	2	1	1	1	1	1	2
2	1	1	1	1	1	1	1	1	1	1	1	1	1	1	1	1	1	2
2	1	1	1	1	1	1	1	1	1	1	1	1	1	1	1	1	1	2
2	2	2	2	2	2	2	2	2	2	2	2	2	2	2	2	2	2	2

Figure B1. Infinite Lattice Configuration

Legend: Figure B1	
🟩	Control Element/Boundary Placeholder
🟦	Fuel Element
🟪	Instrumentation Tube placeholder

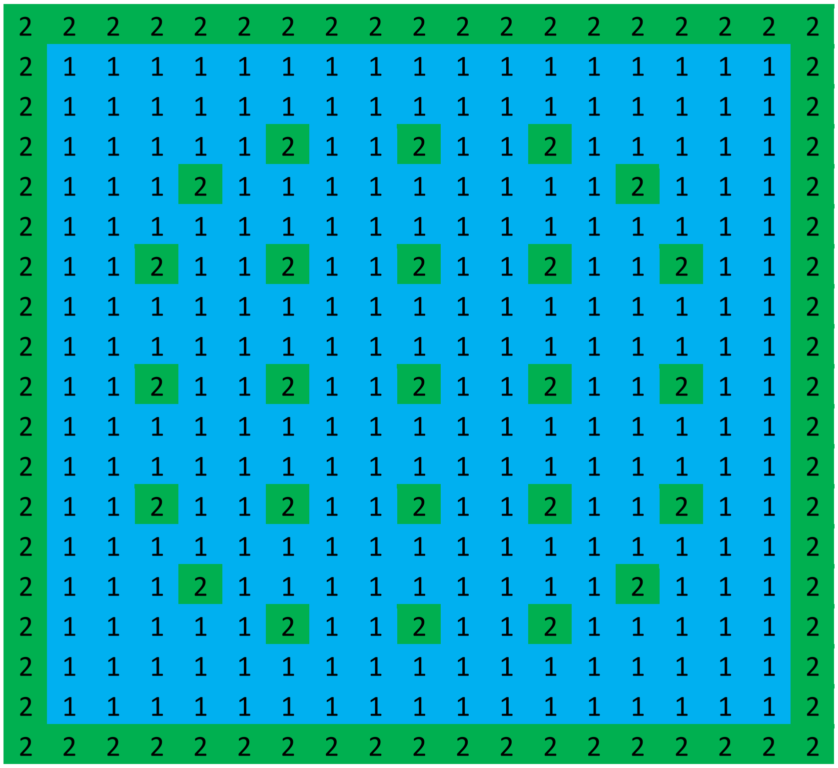

2	2	2	2	2	2	2	2	2	2	2	2	2	2	2	2	2	2	2
2	1	1	1	1	1	1	1	1	1	1	1	1	1	1	1	1	1	2
2	1	1	1	1	1	1	1	1	1	1	1	1	1	1	1	1	1	2
2	1	1	1	1	1	2	1	1	2	1	1	2	1	1	1	1	1	2
2	1	1	1	2	1	1	1	1	1	1	1	1	1	2	1	1	1	2
2	1	1	1	1	1	1	1	1	1	1	1	1	1	1	1	1	1	2
2	1	1	2	1	1	2	1	1	2	1	1	2	1	1	2	1	1	2
2	1	1	1	1	1	1	1	1	1	1	1	1	1	1	1	1	1	2
2	1	1	1	1	1	1	1	1	1	1	1	1	1	1	1	1	1	2
2	1	1	2	1	1	2	1	1	2	1	1	2	1	1	2	1	1	2
2	1	1	1	1	1	1	1	1	1	1	1	1	1	1	1	1	1	2
2	1	1	1	1	1	1	1	1	1	1	1	1	1	1	1	1	1	2
2	1	1	2	1	1	2	1	1	2	1	1	2	1	1	2	1	1	2
2	1	1	1	1	1	1	1	1	1	1	1	1	1	1	1	1	1	2
2	1	1	1	2	1	1	1	1	1	1	1	1	1	2	1	1	1	2
2	1	1	1	1	1	2	1	1	2	1	1	2	1	1	1	1	1	2
2	1	1	1	1	1	1	1	1	1	1	1	1	1	1	1	1	1	2
2	1	1	1	1	1	1	1	1	1	1	1	1	1	1	1	1	1	2
2	2	2	2	2	2	2	2	2	2	2	2	2	2	2	2	2	2	2

Figure B2. Generic PWR Assembly with and without Control Elements

Legend: Figure B2	
🟩	Control Element/Boundary Placeholder
🟦	Fuel Element

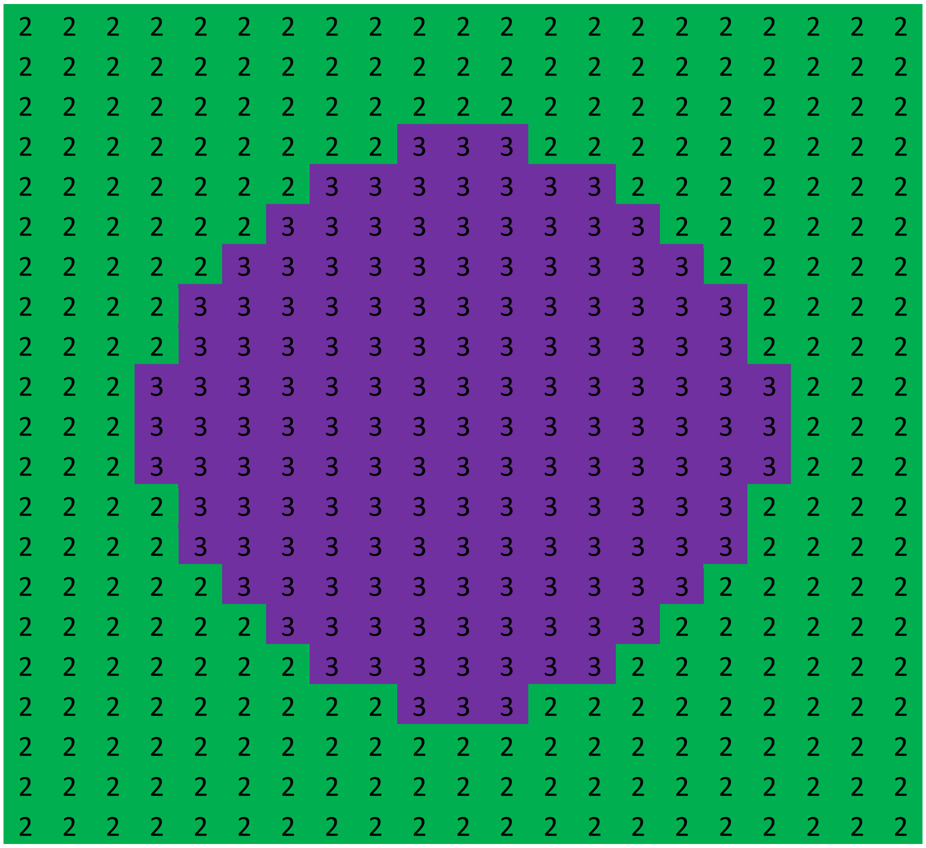

2	2	2	2	2	2	2	2	2	2	2	2	2	2	2	2	2	2	2	2	2
2	2	2	2	2	2	2	2	2	2	2	2	2	2	2	2	2	2	2	2	2
2	2	2	2	2	2	2	2	2	2	2	2	2	2	2	2	2	2	2	2	2
2	2	2	2	2	2	2	2	2	3	3	3	2	2	2	2	2	2	2	2	2
2	2	2	2	2	2	2	3	3	3	3	3	3	3	2	2	2	2	2	2	2
2	2	2	2	2	2	3	3	3	3	3	3	3	3	3	2	2	2	2	2	2
2	2	2	2	2	3	3	3	3	3	3	3	3	3	3	3	2	2	2	2	2
2	2	2	2	3	3	3	3	3	3	3	3	3	3	3	3	3	2	2	2	2
2	2	2	2	3	3	3	3	3	3	3	3	3	3	3	3	3	2	2	2	2
2	2	2	3	3	3	3	3	3	3	3	3	3	3	3	3	3	3	2	2	2
2	2	2	3	3	3	3	3	3	3	3	3	3	3	3	3	3	3	2	2	2
2	2	2	3	3	3	3	3	3	3	3	3	3	3	3	3	3	3	2	2	2
2	2	2	2	3	3	3	3	3	3	3	3	3	3	3	3	3	2	2	2	2
2	2	2	2	3	3	3	3	3	3	3	3	3	3	3	3	3	2	2	2	2
2	2	2	2	2	3	3	3	3	3	3	3	3	3	3	3	2	2	2	2	2
2	2	2	2	2	2	3	3	3	3	3	3	3	3	3	2	2	2	2	2	2
2	2	2	2	2	2	2	3	3	3	3	3	3	3	2	2	2	2	2	2	2
2	2	2	2	2	2	2	2	2	3	3	3	2	2	2	2	2	2	2	2	2
2	2	2	2	2	2	2	2	2	2	2	2	2	2	2	2	2	2	2	2	2
2	2	2	2	2	2	2	2	2	2	2	2	2	2	2	2	2	2	2	2	2
2	2	2	2	2	2	2	2	2	2	2	2	2	2	2	2	2	2	2	2	2

Figure B3. Generic PWR Core Layout without Control Elements

Legend: Figure B3	
🟩	Boundary Cell (Water)
🟪	Fuel Assembly

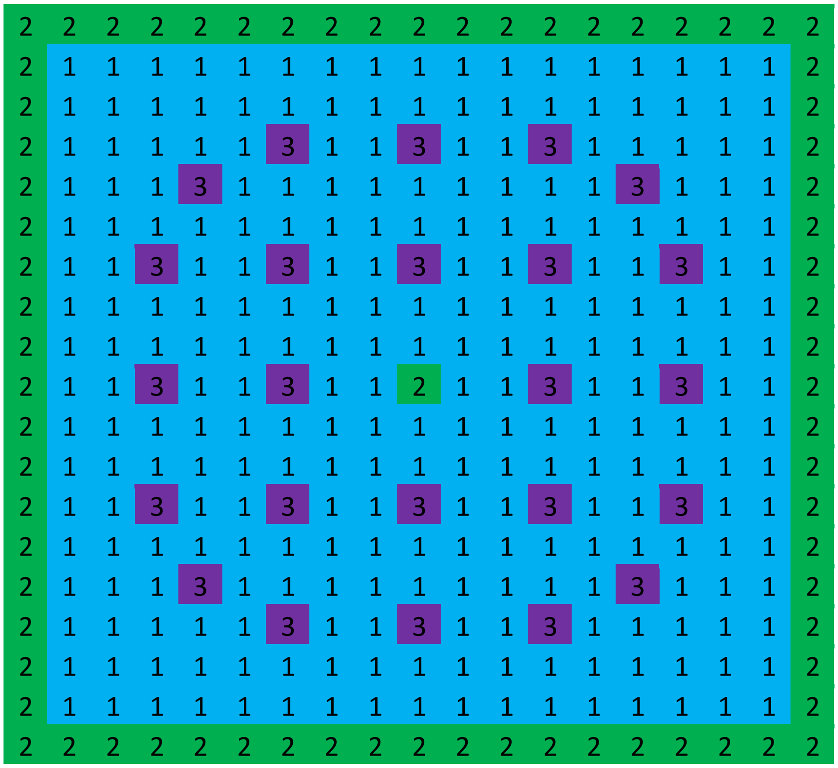

2	2	2	2	2	2	2	2	2	2	2	2	2	2	2	2	2	2	2
2	1	1	1	1	1	1	1	1	1	1	1	1	1	1	1	1	1	2
2	1	1	1	1	1	1	1	1	1	1	1	1	1	1	1	1	1	2
2	1	1	1	1	1	3	1	1	3	1	1	3	1	1	1	1	1	2
2	1	1	1	3	1	1	1	1	1	1	1	1	1	3	1	1	1	2
2	1	1	1	1	1	1	1	1	1	1	1	1	1	1	1	1	1	2
2	1	1	3	1	1	3	1	1	3	1	1	3	1	1	3	1	1	2
2	1	1	1	1	1	1	1	1	1	1	1	1	1	1	1	1	1	2
2	1	1	1	1	1	1	1	1	1	1	1	1	1	1	1	1	1	2
2	1	1	3	1	1	3	1	1	2	1	1	3	1	1	3	1	1	2
2	1	1	1	1	1	1	1	1	1	1	1	1	1	1	1	1	1	2
2	1	1	1	1	1	1	1	1	1	1	1	1	1	1	1	1	1	2
2	1	1	3	1	1	3	1	1	3	1	1	3	1	1	3	1	1	2
2	1	1	1	1	1	1	1	1	1	1	1	1	1	1	1	1	1	2
2	1	1	1	3	1	1	1	1	1	1	1	1	1	3	1	1	1	2
2	1	1	1	1	1	3	1	1	3	1	1	3	1	1	1	1	1	2
2	1	1	1	1	1	1	1	1	1	1	1	1	1	1	1	1	1	2
2	1	1	1	1	1	1	1	1	1	1	1	1	1	1	1	1	1	2
2	2	2	2	2	2	2	2	2	2	2	2	2	2	2	2	2	2	2

Figure B4. Generic PWR Control Assembly Layout

Legend: Figure B4	
🟩	Placeholder Cell (Water)
🟦	Fuel Element
🟪	Control element

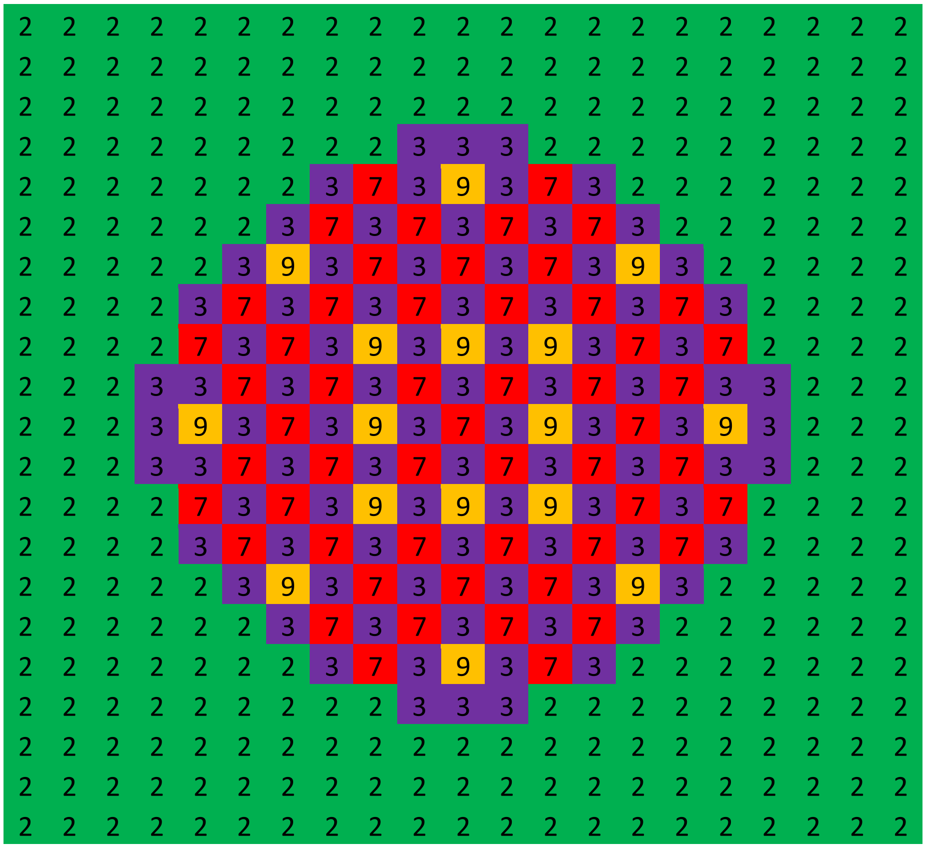

2	2	2	2	2	2	2	2	2	2	2	2	2	2	2	2	2	2	2	2	2
2	2	2	2	2	2	2	2	2	2	2	2	2	2	2	2	2	2	2	2	2
2	2	2	2	2	2	2	2	2	2	2	2	2	2	2	2	2	2	2	2	2
2	2	2	2	2	2	2	2	2	3	3	3	2	2	2	2	2	2	2	2	2
2	2	2	2	2	2	2	3	7	3	9	3	7	3	2	2	2	2	2	2	2
2	2	2	2	2	2	3	7	3	7	3	7	3	7	3	2	2	2	2	2	2
2	2	2	2	2	3	9	3	7	3	7	3	7	3	9	3	2	2	2	2	2
2	2	2	2	3	7	3	7	3	7	3	7	3	7	3	7	3	2	2	2	2
2	2	2	2	7	3	7	3	9	3	9	3	9	3	7	3	7	2	2	2	2
2	2	2	3	3	7	3	7	3	7	3	7	3	7	3	7	3	3	2	2	2
2	2	2	3	9	3	7	3	9	3	7	3	9	3	7	3	9	3	2	2	2
2	2	2	3	3	7	3	7	3	7	3	7	3	7	3	7	3	3	2	2	2
2	2	2	2	7	3	7	3	9	3	9	3	9	3	7	3	7	2	2	2	2
2	2	2	2	3	7	3	7	3	7	3	7	3	7	3	7	3	2	2	2	2
2	2	2	2	2	3	9	3	7	3	7	3	7	3	9	3	2	2	2	2	2
2	2	2	2	2	2	3	7	3	7	3	7	3	7	3	2	2	2	2	2	2
2	2	2	2	2	2	2	3	7	3	9	3	7	3	2	2	2	2	2	2	2
2	2	2	2	2	2	2	2	2	3	3	3	2	2	2	2	2	2	2	2	2
2	2	2	2	2	2	2	2	2	2	2	2	2	2	2	2	2	2	2	2	2
2	2	2	2	2	2	2	2	2	2	2	2	2	2	2	2	2	2	2	2	2
2	2	2	2	2	2	2	2	2	2	2	2	2	2	2	2	2	2	2	2	2

Figure B5. Generic PWR Core Layout with Control Assemblies

Legend: Figure B5	
🟩	Boundary Cell
🟪	Fuel Assembly
🟥	Black Control Assembly
🟨	Gray Control Assembly

Table B1. PWR Model Parameters and Dimensions [Lahoda et al, 2015]

System Temperature	573 K
System Pressure	155 Bar/2248 psi
Fuel Assemblies	157
Arrangement	17x17 square array
Fuel elements per assembly	264
Fuel element cladding OD	0.950 cm
Fuel element cladding thickness	0.057 cm
Fuel element diameter	0.820 cm
Gap thickness (helium)	0.002 cm
Core Height	400 cm
Active Fuel Height	366 cm
Fuel Cladding	Westinghouse ZIRLO
Control Assemblies	63 black; 15 gray
Black rod assembly	24 black rods
Black rod	80-15-5 AIC
Black rod length	360 cm
Gray rod assembly	24 gray rods
Gray rod	12 AIC, 12 SS304 rodlets
Gray rodlet length	15 cm
Control rod cladding	SS 304
Control rod cladding OD	0.967 cm
Control rod cladding thickness	0.046 cm
Rod/rodlet diameter	0.866 cm
Gap thickness (helium)	0.003 cm

REFERENCES

Abdelrazek, I., & Zidan, W. (2002). *Apparent Chemical Reactions Kinetics of the Ammonium Diuranate Precipitation.* Cairo: Atomic Energy Authority.

Braase, L., & May, W. (2014). *Advanced Fuels Campaign FY 2014 Accomplishments Report.* Idaho National Laboratory. United States: Department of Energy. doi:10.2172/1169217

Bragg-Sitton, S., Merrill, B., Teague, M., Ott, L., Robb, K., Farmer, M., . . . Brown, N. (2014). *Advanced Fuels Campaign Light Water Reactor Accident Tolerant Fuel Performance Metrics.* Idaho National Laboratory. US Department of Energy.

Caplan, K. J., Edwards, R. M., Fellows, J. A., Harrington, C. D., Kuhlman, C. W., Philoon, W. C., . . . Shepardson, J. U. (1959). *Uranium Production Technology.* (C. D. Harrington, & A. E. Ruehle, Eds.) Princeton: D. Van Nostrand Company.

Chinthaka Silva, G. W., Yeamans, C. B., Ma, L., Cerefice, G. S., Czerwinski, K. R., & Sattelberger, A. P. (2008). Microscopic Characterization of Uranium Nitrides Synthesized by Oxidative Ammonolysis of Uranium Tetrafluoride. *Chemistry of Materials*, 3076-3084.

Choi, J., Ebbinghaus, B., & Meier, T. (2006). *Laboratory Directed Research and Development on Mono Uranium Nitride Fuel Development for SSTAR and Space Applications.* Lawrence Livermore National Laboratory.

Crane, J., Kalish, H. S., & Litton, F. B. (1962). *The Development of Uranium Carbide as a Nuclear Fuel.* White Plains: United Nuclear Corp. doi:10.2172/4721743

Fane, A., & Le Page, A. (1975). *The Production of Sinterable Uranium Dioxide from Ammonium Diuranate part iii, Continuous Production in a Pulsed Fluidized Bed Reactor*. Lucas Heights: Australian Atomic Energy Commission.

Franceschini, F., Godfrey, A.T., &Gehin, J.C. (2014). AP1000 PWR Reactor Physics Analysis with VERA-CS and KENO-VI Part I: Zero Power Physics Tests. Cranberry Township: Westinghouse Electric Company.

Gordon, E., Dubovitskii, V., Matyushenko, V., Sizov, V., & Kolesnikov, Y. (2006). Uranium Hexafluoride Reduction with Hydrogen Atoms. *Kinetics and Catalysis, 47*(1), 148-156. doi: 10.1134/S0023158406010204

Harp, J. M. (2015, November). Uranium Silicide Pellet Fabrication by Powder Metallurgy for Accident Tolerant Fuel Evaluation and Irradiation. *Journal of Nuclear Materials, 466,* pp. 728-738. doi:10.1016/j.jnucmat.2015.06.027

Jones, R. W., & Croshwaite, J. L. (1973). Uranium Carbide Fuel for Organic Cooled Reactors. Pinawa: Atomic Energy of Canada Limited.

Korea Atomic Energy Research Institute. (2016). *Table of Nuclides*. Retrieved from http://atom.kaeri.re.kr/nuchart/

Lahoda, E., & Boylan, F. (2015). *Development of LWR Fuels with Enhanced Accident Tolerance.* United States: US Department of Energy.

Lightbridge. (2016). *Metallic Fuel Technology.* Retrieved from http://www.ltbridge.com/fueltechnology/metallicfueltechnology

Maloy, S. A., McClellan, K., & Hayes, S. (2014). *Fuel Cycle Research and Development: Advances in Nuclear Fuel and Materials.* United States. Retrieved from http://www.purdue.edu/discoverypark/energy/assets/pdfs/2014%20Nuclear%20Workshop/Maloy_Stuart_PurdueWkshop-10-14.pdf

Matthews, R., Chidester, K., Hoth, C., Mason, R., & Petty, R. (1988, February). Fabrication and testing of uranium nitride fuel for space power reactors. *Journal of Nuclear Materials, 151*(3), p. 345. doi:10.1016/0022-3115(88)90029-3

Malkki, P. (2015). *The Manufacturing of Uranium Nitride for Possible Use in Light Water Reactors.* Stockholm: Royal Institute of Technology.

McDonell, W. R., Caskey, G. R., & Angerman, C. L. (n.d.). *High Performance Uranium Metal Fuels for Savannah River Reactors.* IAEA, Vienna. Retrieved from https://www.iaea.org/OurWork/ST/NE/NEFW/Technical-Areas/RRS/documents/mo99/S_River_Rx_Fuel_Slugs.pdf

McClellan, K. J. (2014). *FY 2014 Ceramic Fuel Development Annual Highlights.* Department of Energy: FCRD Program. United States: Los Alamos National Laboratory. Retrieved from http://permalink.lanl.gov/object/tr?what=info:lanl-repo/lareport/LA-UR-14-27363#page=38

McClellan, K. J. (2015). *FY2015 Ceramic Fuels Development Annual Highlights.* Los Alamos National Laboratory.

Muromura, T., & Tagawa, H. (1977, December). Formation of uranium mononitride by the reaction of uranium dioxide with carbon in ammonia and a mixture of hydrogen and nitrogen— I synthesis of high purity UN. *Journal of Nuclear Materials, 71*(1), 65-72. doi:10.1016/0022-3115(77)90187-8

Muromura, T., & Tagawa, H. (1979, May). Formation of uranium mononitride by the reaction of uranium dioxide with carbon in ammonia and a mixture of hydrogen and nitrogen: II. Reaction rates. *Journal of Nuclear Materials, 80*(2), pp. 330-338. doi:10.1016/0022-3115(79)90196-X

Myerson, A., & Chludzinski, J. (1981). Chemical Kinetics of the Gas-Phase Reaction between Uranium Hexafluoride and Hydrogen. *Journal of Physical Chemistry, 85*(25), 3905-3911.

Nuclear Regulatory Commission. (2010). Module 5.0: Fuel Fabrication. *USNRC Technical Training Center: Fuel Cycle Processes*. United States. Retrieved from http://pbadupws.nrc.gov/docs/ML1204/ML12045A009.pdf

Nuclear Regulatory Commission. (2012). Reactor Core & Vessel Design, AP1000 Technology Chapter 2.0.*Human Resources Training and Development*. United States. Retrieved from http://pbadupws.nrc.gov/docs/ ML1122/ML11221A080.pdf

Puide, M. (2015). High Density Fuels: OECD-NEA EGATFL 3rd Meeting. Sweden. Retrieved from https://www.oecd-nea.org/download/atf-public/ATF2015March-public/documents/TF2-TF3%207.2%20-%20Puide%20-%20High%20Density%20Fuels%20M%20Puide%20Westinghouse-srt.pdf

Rama Rao, G.A., Mukerjee, S.K. Vaidya, V.N., Venugopal, V.,& Sood,D.D. (1991). Oxidation and Hydrolysis Kinetic Studies on UN. *Journal of Nulcear Materials (185), 231-241.*

R.W., K. (1967). Plutonium and Uranium Hexafluoride Hydrolysis Kinetics. *Industrial Engineering Chemical Processes Design and Development, 6*(1), pp. 105-111. doi:10.1021/i260021a018

Saliba Silva, A. M., Durazzo, M., Urano de Carvalho, E. F., & Riella, H. G. (2008, August). Fabrication of U3Si2 Powder for Fuels Used in IEA-R1 Nuclear Research Reactor. *Materials Science Forum, 591-593,* pp. 194-199. doi:10.4028/www.scientific.net/MSF.591-593.194

Saliba-Silva, A. (2011). *Research Reactor Fuel Fabrication to Produce Radioisotopes, Radioisotopes-Applications in Physical Science.* InTech. Retrieved from http://cdn.intechopen.com/pdfs-wm/21643.pdf

Saliba-Silva, A., Aguiar, B., Carvalho, E., Da Silva, D., Riella, H. G., & Durazzo, M. (2011). Analysis of Slag Formation During UF4 Magnesiothermic Reduction. *International Meeting on Reduced Enrichment for Research and Test Reactors.* Santiago.

World Nuclear Association. (2016). *Outline History of Nuclear Energy*. Retrieved from World Nuclear Association Website: http://www.world-nuclear.org/information-library/current-and-future-generation/outline-history-of-nuclear-energy.aspx

Yeamans, C. B., Chinthaka Silva, G. W., Cerefice, G. S., Czerwinski, K. R., Hartmann, T., Burrell, A., & Sattelberger, A. P. (2008). Oxidative Ammonolysis of Uranium(IV) Fluorides to Uranium Nitride. *Journal of Nuclear Materials*, 75-78.

VITA

Benjamin Joseph Prewitt was born in St. Louis, Missouri on November 14, 1991. He received a Bachelor of Science degree in nuclear engineering in May 2014 from the Missouri University of Science and Technology. In the summer of 2014, he was sponsored by the American Nuclear Society to participate in the Washington Internships for Students of Engineering program. There he conducted policy research related to the recycling of nuclear fuel. At the conclusion of that program he enrolled in the nuclear engineering graduate program at the Missouri University of Science and Technology pursuing an M.S. degree. He received a Master of Science degree in nuclear engineering in May 2017.